# Study and Performance Analysis of InAlN/AlN/GaN based Gate Recessed HEMT

**THESIS SUBMITTED IN PARTIAL FULFILLMENT OF THE REQUIREMENTS FOR THE DEGREE OF**

**M.E.**

**IN**

**ELECTRONICS AND TELECOMMUNICATION ENGINEERING**

**BY**

**SRISHTI SRIVASTAVA**

**REGISTRATION NO. – 128926 OF 2014-15**

**EXAM ROLL NO. – M4ETC1612**

**CLASS ROLL NO. – 001410702015**

**UNDER THE SUPERVISION OF**

**Prof. (Dr.) CHANDAN KUMAR SARKAR**

**DEPARTMENT OF ELECTRONICS AND TELECOMMUNICATION ENGINEERING**

**JADAVPUR UNIVERSITY**

**KOLKATA-700 032**

# FACULTY OF ENGINEERING & TECHNOLOGY

# JADAVPUR UNIVERSITY

## CERTIFICATE

This is to certify that the dissertation entitled **"Study and Performance analysis of InAlN/AlN/GaN based Gate Recessed HEMT"** has been carried out by **SRISHTI SRIVASTAVA (University Registration No.: 128926 OF 2014-15)** under my guidance and supervision and be accepted in partial fulfillment of the requirements for the degree of Master of Engineering in Electronics and Telecommunication Engineering of Jadavpur University. The research results presented in the thesis have not been submitted to any other University/Institute for the award of any Degree or Diploma.

_____

**(Prof. (Dr.) Chandan Kumar Sarkar)**

Project Supervisor
Department of Electronics &
Telecommunication Engineering
Jadavpur University
Kolkata 700 032

**COUNTERSIGNED**

_____

**(Prof. Palaniandavar Venkateswaran)**

Head, Department of Electronics &

Telecommunication Engineering,

Jadavpur University

Kolkata – 700 032

_____

**(Prof. Sivaji Bandyopadhyay)**

Dean, Faculty of

Engineering & Technology,

Jadavpur University

Kolkata – 700 032

# FACULTY OF ENGINEERING & TECHNOLOGY

# JADAVPUR UNIVERSITY

**DEPARTMENT OF ELECTRONICS AND TELECOMMUNICATION ENGINEERING**

## CERTIFICATE OF APPROVAL

The foregoing thesis is hereby approved as a creditable study of an engineering subject, carried out and presented in a manner satisfactory to warrant its acceptance as a prerequisite to the degree for which it has been submitted. It is understood that by this approval the undersigned do not necessarily endorse or approve any statement made, opinion expressed or conclusion drawn therein but approve the thesis only for the purpose for which it has been submitted.

**Committee on final examination**

**for the evaluation of the Thesis**

_____ _____

Signature of the Examiner Signature of the Supervisor

*Only in case the thesis is approved

# FACULTY OF ENGINEERING & TECHNOLOGY

# JADAVPUR UNIVERSITY

## ***DECLARATION OF ORIGINALITY AND COMPLIANCE OF ACADEMIC THESIS***

I hereby declare that this thesis titled **"Study and Performance analysis of InAlN/AlN/GaN based Gate Recessed HEMT"** contains literature survey and original research work by the undersigned candidate, as a part of his degree of **Master of Electronics and Telecommunication Engineering of Jadavpur University.**

All information have been obtained and presented in accordance with academic rules and ethical conduct.

I also declare that, as required by these rules and conduct, I have fully cited and referenced all the materials and results that are not original to this work.

| | | |
|---|---|---|
| **Name** | : | SRISHTI SRIVASTAVA |
| **Examination Roll No** | : | M4ETC1612 |
| **Thesis Title** | : | STUDY AND PERFORMANCE ANALYSIS OF InAlN/AlN/GaN BASED GATE RECESSED HEMT |
| **Signature** | : | |
| **Date** | : | |

Dedicated to

My Parents for their unconditional love, support and encouragement

# ACKNOWLEDGEMENT

There are many people I would like to thank for their indispensable support to me for winding up this thesis. First of all, I would like to express my sincere gratitude to my supervisor Professor Chandan Kumar Sarkar for inspiring me with his knowledge, enthusiasm, and wisdom in semiconductors. I am enormously obliged to him as under his guidance my knowledge in the field of semiconductors expanded from the day when I first joined the M.E. Course to evolve into a device modeler.

I am grateful to Mr. Sanjit Kumar Swain, QIP fellow, Jadavpur University for his crucial suggestion and guidance that helped me in successful conclusion of the work.

I would like to thank Dr. Chayanika Bose, Professor, Jadavpur University for her extraordinary teachings, valuable advice and motivation when I was a beginner in the field of advanced semiconductor physics.

I would like to thank Mr. Sarosij Adak, Senior Research Fellow, School of VLSI Technology, Indian Institute of Engineering Science and Technology for his altruistic help extended to me for understanding the Sentaurus TCAD simulator and SILVACO and I will always cherish the discussions we had. It

will also be very unappreciative of me to not thank Mr. Bikash Sharma, QIP fellow, Jadavpur University for his endless support, guidance and discussions that enlightened me.

Finally I would like to thank my parents, my siblings and my friends for their unconditional love, support and blessings which have brightened up my life in every possible way I can think of.

Srishti Srivastava
Dept. of ETCE
Jadavpur University

# *List of Publications*

1. "**Performance Analysis of T-gate Enhancement mode n++ GaN/InAlN/AlN/GaN HEMT**", Srishti Srivastava, Sanjit Kumar Swain, Sarosij Adak, Chandan Kumar Sarkar, **ICIIECS '16**, Coimbatore (to be published in IEEE explore), India.

2. "**Microwave characteristics of 100nm AlGaN Back barrier Gate Recessed Enhancement mode InAlN/AlN/GaN HEMT**" Srishti Srivastava, Sanjit Kumar Swain, Sarosij Adak, Chandan Kumar Sarkar, **ICIIECS '16**, Coimbatore (to be published in IEEE explore), India.

# Abstract

*The performance of devices using conventional semiconductors such as Si and GaAs is rapidly approaching the limit set by intrinsic material parameters. The increasing demand for high power at high frequency has led to the development of microwave power devices in wide band gap material systems such as GaN and SiC. In this work the impact of Drain voltage, doping concentration of cap layer and channel length on the performance of 100nm T-gate $n^{++}$GaN/InAlN/AlN/GaN Enhancement mode HEMT is studied. AlInN/GaN heterostructure have substantially higher spontaneous polarization induced 2DEG density. The lattice matching reduces the stress in the barrier layer, which leads to improved linearity.*

*In this work RF and Analog performance of the new 100nm T-gate $n^{++}$GaN/InAlN/AlN/GaN Enhancement mode HEMT device is comprehensively investigated using 2D Sentaurus TCAD simulations. The result of the model has been found in good agreement with the simulation result. The average error here is near about 1% of the experimental values. T-gate structure is a solution to achieve the desired high frequency performance. Here the introduced T-gate is not recessed one so it overcomes the major SCE restrictions. A very high $f_T$ of the order of 195 GHz and considerably reduced leakage current up to $10^{-5}$ order is the biggest advantage of introduced T-gate. Several other parameters have been discussed in depth.*

**Keywords: SCE, T-Gate, HEMT, TCAD, 2DEG.**

# *List of Tables*

# *List of Figures*

# List of Symbols

| SYMBOLS | DESCRIPTIONS | UNITS |
|---|---|---|
| $V_{th}$ | Threshold Voltage | V |
| $I_d$ | Drain Current | A |
| W | Channel width | nm |
| $g_m$ | Transconductance | ms/mm |
| $g_m/I_d$ | Transconductance Generation Factor | $V^{-1}$ |
| $V_g$ | Gate Voltage | V |
| L | Channel length | nm |
| $I_{off}$ | Gate leakage Current | A/um |
| $N_s$ | Surface Concentration Donor | $cm^{-3}$ |
| $N_A$ | Substrate doping Concentration (donor) | $cm^{-3}$ |
| $V_{gs}$ | Gate to Source Voltage | V |
| $V_{ds}$ | Drain to Source Voltage | V |
| $N_D$ | Source drain acceptor doping Concentration | $cm^{-3}$ |
| $V_{bi}$ | Built in voltage | V |
| $W_d$ | Channel depletion width | nm |
| k | Boltzmann's Constant (1.38 × 10-23) | J/K |
| $N_i$ | Intrinsic Doping Concentration | $cm^{-3}$ |
| $Q_s$ | Total Depletion charge per unit area | $C/cm^2$ |
| $V_{tho}$ | Long Channel Threshold Voltage | V |
| q | Charge (1.6 × 10-19) | C |
| ρ | Charge Density | $C/cm^3$ |
| $N_d^+$ | ionized donor concentrations | $cm^{-3}$ |

| | | |
|---|---|---|
| $N_A^+$ | ionized acceptor concentrations | $cm^{-3}$ |
| $\varepsilon$ | Permittivity | F/cm |
| $\varepsilon_{ox}$ | Permittivity of oxide | F/cm |
| n | electron concentration | $cm^{-3}$ |
| p | hole concentration | $cm^{-3}$ |
| $J_n$ | current density for electrons | $A/cm^2$ |
| $J_p$ | current density for holes | $A/cm^2$ |
| $D_n$ | electron diffusion coefficient | $cm^2/s$ |
| $D_p$ | hole diffusion coefficient | $cm^2/s$ |
| $N_{eff}$ | effective channel doping concentration | $cm^{-3}$ |
| $E_i$ | intrinsic Fermi level | V/cm |
| $f_T$ | cut off frequency | GHz |
| $f_{max}$ | maximum frequency | GHz |
| $H_{21}$ | short circuit current gain | - |
| $dR_s$ | dynamical source access resistance | Ω |

# CONTENTS

# Chapter 1

# Introduction

## 1.1 BACKGROUND

Since the invention of Metal-Oxide-Semiconductor field-effect-transistor (MOS-FET) in 1959, the semiconductor industry for electronics has been dominated by Silicon (Si). This is mainly because of easy availability, low cost and ease of creating a native oxide on Si. However there are some applications like Light emitting diodes (LED), laser diodes (LDs) and radio frequency (RFs) devices where compound semiconductors have been the workhouse materials. Limited mobility, low band-gap, low breakdown voltage, and low operating temperature limits the current carrying and output power generation capability of silicon based devices.

High power and high frequency requirements in advanced telecommunication systems become more stringent as faster and higher capacity wireless data transfer over long distances is getting a common need for both military and commercial applications. GaN HEMT device technology promises high power performance in microwave and millimetre wave regimes at least an order of magnitude better than any other current counterparts.

The first GaN based transistors were realized in the early to mid-1990's [1,2] and since then have been extensively researched and developed for high-power high-frequency applications as well as for high-voltage power switches. GaN falls into the category of wide band gap semiconductors (Bandgap Energy, $E_g$ = 3.44eV) and it has an ability to form heterojunction to wider gap semiconductors such as aluminium gallium nitride (AlGaN), aluminium indium nitride (AlInN), and aluminium nitride (AlN) (upto 6.2eV). This result in a two-dimensional-electron-gas (2DEG) formed at the interface due to large polarization in the material which provides a highly dense,

majority carrier channel with large electron mobility. These properties can be exploited to make devices which are capable of handling or providing high output power that can be operated as power switches or comfortably up to 10GHz for power amplifier applications respectively.

In addition to the large bandgap the polar nature of GaN crystal gives it an edge over other materials. The 2DEG density in GaN-based devices has been reported to be around and, in many cases, above $10^{13}$ $cm^{-2}$, making it almost six times larger than that of a GaAs HEMT [3]. A higher mobility and electron density leads to higher output current density. Nowadays, an output power density of 30-40 W/mm is achieved which is more than ten times higher than that of GaAs based transistors. Thus, for the same output power, device size can be considerably reduced for GaN based devices [4]. Furthermore, good thermal stability of GaN-based HEMTs allows operation at high temperature.

Compared to other competitive materials like GaAs and SiC, the advantage of GaN rests on wider and direct band-gap (for opto-electronic applications), which allows for short wavelength laser diodes and LEDs [5, 6, 7], and high breakdown voltage (for RF applications) [8].

By 2021 it is expected that GaN devices will have a market valuation of around $1 billion [9]. Yole Development, a group of companies providing market research, technology analysis, strategy consulting, media, and financial services, published a report in July 2012 titled ‘Status of the Power Electronics Industry,’ which outlined their expectation of the trend the power electronics would follow over the coming years. Fig 1.1 is an adaption of a graph which they published showing a

prediction of where the current and future technologies might lie. GaN occupies a very large proportion of this graph and in recent years research into this area has accelerated which can probably be attributed to the realization that the market potential will be so large.

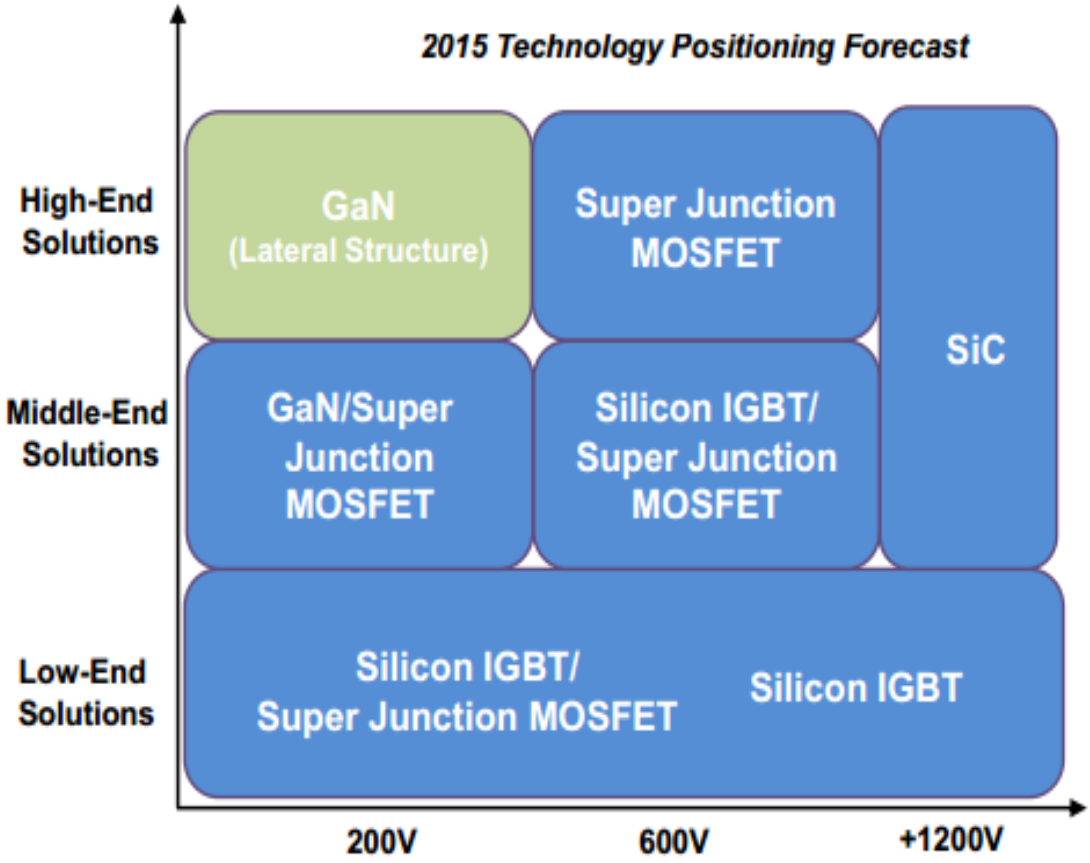


**Figure 1.1: Technology positioning depending on voltage range and system value requirements (This graph is adapted from a report published by Yole Development [9]).**

## 1.2 MOTIVATION FOR THE PRESENT WORK

Due to significantly increasing SCEs because of scaling of MOSFET to sub 20nm dimension, it has now become very difficult to maintain device performance.

Now researchers are focussing on increasing device drive current for rapid switching. This led to large leakage current which results to excessive standby power dissipation [10]. Thus, there is need to investigate new channel materials to meet present researchers requirement i.e. high switching speed and reduced SCEs.

The III-V compound semiconductor binaries such as GaAs, GaN, InP, ternaries such as InGaAs, AlGaAs, AlGaN, AIInN and quaternary InAlGaN, InAlGaAs, GaInPAs are widely studied for enhancing the device performance. The GaAs based compounds have much higher mobility than the silicon and are thus suitable for high speed operation. On the other hand, III-nitride compounds have higher bandgap than the silicon enabling high temperature, high power and high frequency operation. The III-nitride compounds also offer higher breakdown voltage. The heterostructure build using III-V compound semiconductors consist of two or more layer having different bandgap grown one above the other. Such heterostructure leads to the formation of a high mobility quantum well at the hetero interface of the wide bandgap and narrow bandgap semiconductor layers. The charge carriers confined in these quantum wells can move in two dimensions (2D) only and have very high mobility, and are thus termed as two dimensional electron gas (2DEG). The GaN\ heterostructure such as AlGaN/GaN and AlInN/GaN offers a very high 2DEG density without any intentional doping. The absence of doing lead to reduced scattering effects and thus very high mobility can be achieved. These unique features helps to achieve very high drain current density in GaN heterostructure based HEMTs (High Electron Mobility Transistors) and MOS-HEMTs (Metal Oxide Semiconductor High Electron Mobility Transistors). As compared to the conventional AlGaN/GaN heterostructure, the lattice matching in AlInN/GaN

heterostructure avoids strain related problems, provides higher 2DEG density and higher drives currents thus, motivating its use in HEMTs and MOS-HEMTs.

Gallium nitride (GaN) based high electron-mobility transistors (HEMTs) have demonstrated high-power and high-frequency performance thanks to their high electron-saturation velocity and high sheet-carrier density in two-dimensional electron gas (2DEG) [11]. In order to achieve improved high frequency operation the gate length of existing InAlN/GaN HEMT needs to be scaled down. But we already know the reduction in barrier layer thickness will result in reduced short channel effects (SCE). However, the immoderate scaling of the top AlInN barrier layer in these devices causes a remarkable reduction in the two dimensional electron gas (2DEG) density and leads to severe increase in the gate leakage current [12].

T-gate structure is another solution to achieve the desired high frequency performance. T-gate enhancement mode AlInN/GaN HEMT have been seen in the literature [13-14] and have resulted in improved RF performance. In all these structures the T-gate is recessed through the top barrier layer which leads to major SCE restrictions on high frequency performance [15].

From the literature and experimental viewpoints a gate recess plays a significant role in device performance of GaAs [16] and GaN based HFETs [17-18]. It provides an improvement in the transconductance of the structures compared to none recessed ones [19]. A gate recess is also important to reduce source resistance Rs [20] which is useful for high frequency circuits.

T-gate technology is used to improve the device characteristics by reducing the gate resistance at very small gate length. T-gate is a reduction of Rg by increasing the "T" and keeping gate length Lg small at the same time. But at the same time the gate capacitance Cg increases. Therefore the width of the T-gate head must be chosen as a trade-off value between the resistance and the capacitance [21].

S. Adak et al. reported a $f_T$ of 123GHz for the 150nm T-gate recess enhancement mode AlInN/GaN HEMT having less SCE by using p-GaN back barrier concept but drain current is reduced which is a drawback of that device [22]. In 2013, D.M. Geum et al. presented $f_T$ = 170 GHz in a 75nm T-gate AlInN/GaN HEMT [23] and in the same year L. Bo et al demonstrated a 200nm T-gate AlInN/GaN HEMT having $f_T$ of 60 GHz [24], both the device reduced SCE due to the insertion of AlGaN back barrier but these two devices are in depletion mode HEMT which is hard to use for switching application.

In this dissertation, Enhancement mode n++ GaN/InAlN/AlN/GaN HEMT E-mode InAlN/AlN/GaN HEMTs have been considered which support enhancement mode but T-gate is not recessed through AlInN top barrier layer which ensures low SCE, high drain current, and higher cut off frequency, $f_T$. The performance of the said device needs to be investigated systematically for the inspection of its capability for high frequency as well as switching applications. Hence, we have performed the simulations comprehensively to determine the various characteristics (DC and Analog/RF performance) of the device accurately. All these studies would certainly provide valuable insight about the viability of the novel n++

GaN/InAl N/AlN/GaN HEMT E-mode InAlN/AlN/GaN HEMTs for high frequency applications.

## 1.3 ORGANIZATION OF THE THESIS

This dissertation is divided into five main chapters. First chapter starts with the brief discussion on present scenario of GaN device and advantages of InAlN/GaN over AlGaN/GaN. This chapter mainly explains the emerging trend of III-V semiconductors to overcome the problem associated with scaling. The chapter presents the outline of the thesis.

The second chapter provides a brief comparison of the commonly used III-V compound semiconductors. General material and transport properties, advantages, and theoretical electrical and thermal limits of GaN are presented. A brief comparison of the GaN and other semiconductors is included. Advantages of AlInN/GaN over AlGaN/GaN is presented. The material parameters of $Al_{0.83}In_{0.7}N$ and GaN, along with the polarization charges at each interface are listed. Polarization concept has been introduced. Device structure and simulation framework of T-gate $n^{++}$ GaN/InAlN/AlN/GaN Enhancement mode HEMT have been elaborated in this chapter. Fundamental models used in the simulation have been extensively discussed.

Third chapter comprehensively analyses the impact of drain bias voltage and $n^{++}$ GaN cap doping density on analog/RF parameters. Effect on drain current ($I_d$), Transconductance ($g_m$), transconductance generation factor (TGF) ($g_m/I_d$), Gate leakage current have been discussed using simulation. RF performance of the device has been evaluated over a wide frequency range using simulation.

Chapter 4 comprehensively analyses the impact of Gate length on Analog parameters such as drain current ($I_d$), Transconductance ($g_m$), transconductance generation factor (TGF) ($g_m/I_d$), Gate leakage current, Cut off frequency ($f_T$), and maximum frequency ($f_{max}$). Gate length is varied from 75nm to 125nm.

Finally, fifth chapter explains the major conclusion and outcomes of the present work. The chapter ends with some suggestions and directions for future work.

## REFERENCES

[1] M. A. Khan, A. Bhattarai, J. N. Kuznia, and D. T. Olson, "High electron mobility transistor based on a GaN-AlGaN heterojunction," *Applied Physics Letters*, vol. 63, pp. 1214 – 1215, 1993.

[2] M. A. Khan, J. N. Kuznia, D. T. Olson, W. J. Schaff, J. W. Burm, and M. S. Shur, "Microwave performance of a 0.25$\mu$m gate AlGaN/GaN heterostructure field effect transistor," *Applied Physics Letters*, vol. 65, no. 9, pp. 1121 –1123, 1994.

[3] R. J. Trew, "SiC and GaN Transistors—Is there one winner for microwave power applications?", *Proceedings of the IEEE,* Vol. 90, No. 6, 2002.

[4] U. K. Mishra *et al.*, "AlGaN/GaN HEMTs—Overview of device operation and applications", *Proceedings of the IEEE,* Vol. 90, No. 6, 2002.

[5] Nakamura *et al.*, "P-GaN/N-InGaN/N-GaN Double-Heterostructure Blue-LightEmitting Diodes", *Japanese Journal of Applied Physics*, Vol. 32, 1993.

[6] Nakamura, "III-V nitride based light-emitting devices", *Solid State Communications*, Vol. 102,No.2-3,1997.

[7] Sandvik *et al.*, "*AlxGa*1−*xN* for solar-blind UV detectors", *Journal of Crystal Growth*, Vol. 231, No. 3, 2001.

[8] S. Karmalkar, M. S. Shur and R. Gaska, "GaN-based Power High Electron Mobility
Transistors", Chapter 3, *Wide Energy Bandgap Electronic Devices,* World Scientific Publishing Company (2003).

[9] Semiconductor Today, “GaN power electronics market may top $ 1bn in a few years,” accessed March 2013. http://www.semiconductortoday.com/news items/2012/MAR/YOLE 080312.html.

[10] S. Oktyabrsky and D. Ye. Peide, Fundamentals of III–V Semiconductor MOSFETs, 1st ed. Springer, Heidel berg, 2010.

[11] Mishra, U., Shen, L., Kazior, T.E., and Wu, Y.-F.:‘GaN-based RF power devices and amplifiers’, Proc. IEEE., 2008, 96, (2), pp. 287–305 F. Medjdoub, M. Alomari, J.-F. Carlin, M. Gonschorek, E. Feltin, M. A. Py, N. Grandjean, and E. Kohn, “Barrier-layer scaling of InAlN/ GaN HEMTs,” IEEE Electron Device Lett., vol. 29, no. 5, pp. 422–425, May 2008.

[12] R. Wang, P. Saunier, X. Xing, C. Lian, X. Gao, S. Guo, G. Snider, P. Fay, D. Jena, and H. Xing, “Gate-recessed enhancement-mode InAlN/AlN/GaN HEMTs with 1.9 A/mm drain current density and 800 mS/mm transconductance,” IEEE Electron Device Lett., vol. 31, no. 12, pp. 1383–1385, Dec. 2010.

[13] B. Song, B. Sensale-Rodriguez, R. Wang, A. Ketterson, M. Schuette, E. Beam, et al., “Monolithically integrated E/D-mode InAlN HEMTs with $f$t /$f$max > 200/220 GHz,” in Proc. IEEE 70th Annu. DRC, Jun. 2012, pp. 1–2.

[14] B. Song, B. Sensale-Rodriguez, R. Wang, J. Guo, Z. Hu, Y. Yue, F. Faria, M. Schuette, A. Ketterson, E. Beam, P. Saunier, X. Gao, S. Guo, P. Fay, D. Jena, H.G.Xing, "Effect of Fringing Capacitances on the RF Performance of GaN HEMTs With TGates," IEEE Trans Elec. Dev.,, vol.61, no.3, pp.747-754, March 2014.

[15] G. H. Jessen, R. C. Fitch, J. K. Gillespie, G. Via, A. Crespo, D. Langley, D. J. Denninghoff, M. Trejo, and E. R. Heller, “Shortchannel effect limitations on high-frequency operation of AlGaN/GaN HEMTs for T- Gate devices,” IEEE Trans. Electron Devices, vol. 54, no. 10, pp. 2589–2597, Oct. 2007.

[16] M. M. Ahmed. “Effect of active-channel thickness on submicron GaAs metal semiconductor field effect transistor characteristics”.J. Vac. Sci. Technol. B 16(3) page 968-71 (1998)

[17] T. Egawa, H. Ishikawa, M. Umeno and T. Jimbo. “Recessed gate AlGaN/GaN MODFET on sapphire”. Appl. Phys. Lett. Vol 76, No 1, page 121-123 (1999)

[18] S. C.. Binari, K. Doverspike, G. Kelner, H. B. Dietrich and A. E. Wickenden, Solid state electron. 41, 177, (1997)

[19] Franck Stengel, S. Noor Mohammad and H. Morkoç Theoretical investigation of electrical characteristics of GaN/AlGaN modulation doped field-effect transistors. J. Appl. Phys. 80page, 3031-3042 [1996]

[20] Oliver Breitschädel, B. Kuhn, F. Scholz, and H. Schweizer. "Minimization of Leakage Current of Recessed Gate GaN/AlGaN HEMTby optimizing the Dry-Etching Process ". Jour of Elec. Material. Vol 28, No 12, (1999) page, 1420-1423

[21] J. Mateos, T. Gonzalez, D. Pardo, V. Hoel and Alain Cappy. Effect of the T-gate on the performance of recessed HEMTs. A Monte Carlo Analysis. Semicond. Sci. Technol. 14 page 864-870 (1999)

[22] S. Adak, A. Sarkar, S. Swain, H. Pardeshi, S.K. Pati, C.K. Sarkar, "High performance AlInN/AlN/GaN p-GaN back barrier GateRecessed Enhancement-Mode HEMT" Superlattices and Microstructures, vol. 75, pp. 347-357 ,2014.

[23] D. M. Geum et al., "75 nm T-shaped gate for In0.17Al0.83N/GaN HEMTs with minimal short-channel effect," Electron. Lett., vol. 49, no. 24, pp. 1536–1537, Nov. 2013.

[24] Liu Bo , Feng Zhihong , Dun Shaobo , Zhang Xiongwen ,Gu Guodong , Wang Yuangang , Xu Peng , He Zezhao and Cai Shujun. An extrinsic fmax > 100 GHz InAlN/GaN HEMT with AlGaN back barrier. Journal of Semiconductors, 2013, 34(4): 044006.

# *Chapter 2*

# III-V Compound Semiconductors and GaN Physics

## 2.1 INTRODUCTION

This chapter introduces the physical aspects of III-V material concentrating mainly on GaN, its material properties and polarization effects. For a systematic introduction Figure 2.1 depicts the bandgap at a lattice temperature of 300K for various semiconductor materials as a function of lattice constant. With the bandgap of InN recently suggested to be about 0.8eV and the bandgap of AlN to be 6.2 eV at room temperature, the III-N material system covers a very broad range of energies and thus emission wave lengths from the infrared to the deep ultraviolet unchallenged by any other available material. Electronically, a very broad range of bandgap energies is found resulting in extremely high bulk material breakdown voltages, which can be traded in for low-effective mass and high mobility of GaN with $m_n = 0.2\ m_e$, or even of InN with $m_n = 0.11\ m_e$ (potentially even $m_n = 0.04 m_e$ [1]) by changing the material compositions in the heterostructure.

At the same time, a second trade-off is imminent and different from any other semiconductor material system i.e. polarization concept. Due to the strong polar material properties, the modification of the material composition results in dramatic modifications of the polar material properties, and thus of available carrier concentrations obtained at the interfaces. Thus, the huge success of III-V material is not mainly due to the intrinsic bulk material transport properties, but due to the interface properties. In the case of Silicon, the success is based on the formation of a native oxide which can be optimized and used tremendously [2], and is recently replaced by other dielectrics, which also well behave as silicon [3, 4]. In the case of III-V heterostructure, the interfaces allow for the

formation of n-channels and intrinsically provide extremely high carrier concentrations of the order of $10^{13}$ $cm^{-2}$ through polarization engineering without further impurity doping.

Thus III-V compound semiconductors have become a promising alternative for microwave power device. They have demonstrated excellent performance in such applications as UV detectors, UV and visible light emitting diodes (LEDs), microwave power amplifications, satellite, radar and wireless communication systems.

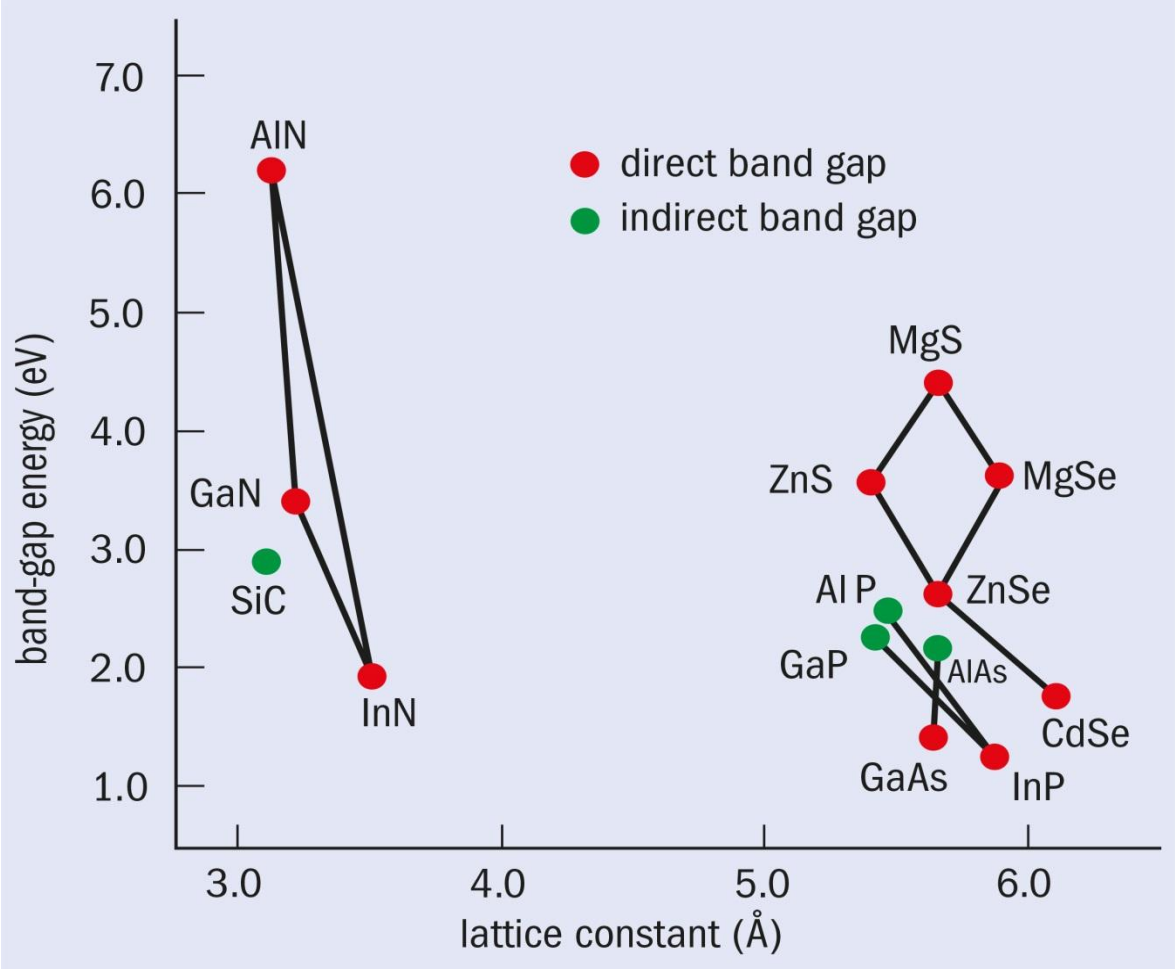


**Figure 2.1: Bandgap energy at TL=300K as a function of lattice constant of III-N semiconductors. Other III-V semiconductors are given for comparison.**

Section 2.2 provides an overview of structural properties of GaN leading to a discussion in chapter introduces the physical aspects of III-nitride materials concentrating on polarization effects. A thorough comparison of electrical properties of various III-V compound semiconductors has been made in section 2.3

## 2.2 GaN: STRUCTURAL PROPERTIES

**The III-N semiconductors can be found in three common crystal structures :**

1. Wurtzite
2. Zincblende
3. Rock salt

At room temperature GaN, AlN, and InN are found in the wurtzite structure, while BN prevails mostly in the cubic structure. The zincblende structure can also be found for GaN and InN for thin films, while for AlN no stable zinc blende phase has yet been detected [5]. In the wurtzite structure the growth is typically performed along the *c*-axis. Recently, growth along the m-plane has been reported [6, 7] as the resulting nonpolar material has a positive influence on diodes efficiency in optoelectronics.

Among wurtzite and Zinc Blende Structure Wurtzite is found to be a more stable structure. As a result of this inherent stability, wurtzite HCP is preferred for fabricating devices. The wurtzite crystal structure has four atoms per unit cell in a hexagonal Bravais lattice [8]. The three lattice parameters are the length of a side of the hexagonal base, *a*, the height, *c* and the III-N bond length along the *c*-axis, *u*.

Crystals with non-Centro-symmetric structure, like GaN, show different layer sequencing of atoms when one moves from one side of the crystal to the other in opposite directions. The GaN wurtzite HCP structure shows this crystallographic polarity along the *c*-axis (perpendicular to the basal plane of GaN crystal structure [9]. It is in this direction that Ga and N atoms arrange themselves in atomic bilayers. These bilayers consist of two closely spaced hexagonal layers, formed by Ga (cation) and N (anion), resulting into polar faces due to the electronegativity difference between composite atoms (Ga-and N- face) [9]. Polarization is a macroscopic material property in which difference in electronegativity between atoms making bonds with each other results in the shift of positive and negative charge centers. This polarization of atomic bonds leads to the creation of dipoles with dipole moments whose direction depends on the type of bonding atoms [10]. In the absence of any electric field, orientation of these dipoles is random and the net polarization is zero. But in the case of GaN, which lacks symmetry in *c*-axis, the presence of an inherent electric field due to asymmetry can result in the formation and subsequent maintenance of a permanent dipole moment which results in polarization of the material. This kind of polarization is called ***Spontaneous polarization*** as it does not require any external force like electric field or deformation.

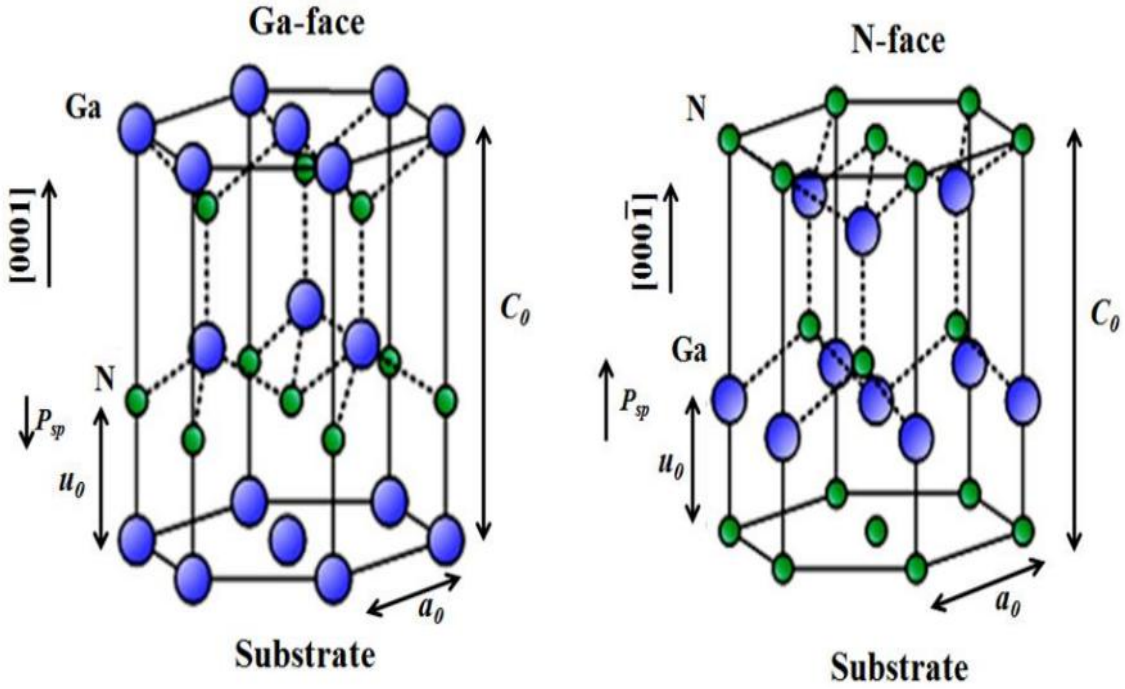


**Fig. 2.2 Schematic of the wurtzite Ga-face and N-face GaN. The direction of spontaneous polarization ($P_{sp}$) is also shown**

## 2.3 GaN Electrical Properties

Over the last decades, GaN has been very promising research topic and candidate for high power applications due to its superior material properties over conventional ones. Table 2.1 represents important material properties of GaN and some other semiconductors. GaN is a wide bandgap material and thereby it can withstand very high temperature and even voltage [11], [12], [13], [14]. Radiation hardness of the GaN is comparable with SiC and higher than GaAs [15]. Thermal Conductivity of GaN is significantly higher than that of GaAs. This makes GaN more suitable for high power operations as compared to GaAs power devices. GaN is at a better position than its

competitors because of its high saturated electron drift velocity than that of Si, SiC, GaAs.

GaN is very stiff material that makes it mechanically easy to handle. Moreover it has an advantage of being stable even at very high temperatures even upto 1200$^{o}$C under atmospheric pressures [16].

The dielectric constant simply indicates the capacitive loading capability of a transistor and so it affects the device terminal impedances [17]. As compared to conventional semiconductors the dielectric constant of wide band-gap semiconductors is about 20% lower which permit them to be about 20% larger in area for given impedance. Increased area allows for higher RF currents, and therefore higher RF power. The critical electrical field for electronic breakdown is an indication of the strength of the electric fields that can be supported internally by the device before breakdown. Higher electric field permits for generation of high RF power. As we have already discussed the bandgap of III-Nitride material is very high which results in high breakdown electric field (3.3 MV/cm). In addition, if they are grown on high conductivity substrates like SiC, it adds up to its good thermal conduction properties.

Bandgap and other electrical properties can by computed by using Vegard's law given by-

$$\mathbf{P\,(}\mathit{AlxGa1\text{-}xN}\mathbf{) = x\,P(}\mathit{AlN}\mathbf{) + (1\text{-}x)\,P\,(}\mathit{GaN}\mathbf{) + b\,x(}\mathit{1\text{-}x}\mathbf{)} \qquad \mathbf{(2.1)}$$

Where P(x) represents the electrical property to be interpolated and b represents the bowing parameter which has to be experimentally determined for accurate

interpolation. As we know mobility of the charge carriers given by ration of carrier velocity and applied electric fields decides the current flowing in the device. If we look at the carrier velocity Vs. Electric field characteristics for various semiconductors shown in fig 2.3, we observe that the carrier velocity is comparatively high for GaN and its peak velocity is observed at very high electric fields. Although mobility of GaN for low fields is not as high as GaAs, the current is still high due to high 2DEG density which will be explained in the upcoming section.

| **Property** | **Si** | **GaAs** | **4H-SiC** | **6H-SiC** | **GaN** |
|---|---|---|---|---|---|
| Bandgap, (eV) | 1.12 | 1.42 | 3.27 | 3.02 | 3.4 |
| Breakdown Electric Field, (MV/cm) | 0.3 | 0.4 | 3 | 3.2 | 3.3 |
| Relative dielectric constant | 11.7 | 12.9 | 9.7 | 9.66 | 8.9 |
| Thermal Conductivity $\kappa$, (W/cm·K) | 1.3 | 0.55 | 3.7 | 4.9 | 1.3 |
| Electron Mobility $\mu_n$ , ($cm^2$/V·s) | 1400 | 8500 | 900 | 400 | 1000 |
| Hole Mobility, ($cm^2$/V·s) | 450 | 400 | 120 | 90 | 200 |
| Saturated Electron Drift Velocity, ($x10^7$ cm/s) | 1 | 1 | 2 | 2 | 2.5 |
| Melting Point, K | 1415 | 1238 | 2827 | | 2791 |

**Table 2.1 Material properties and figures of merit (FOM) of GaN, 4H-Sic, GaAs and Si at 300K for microwave power device application. All FOMs are normalized with respect to those of Si [12].**

The frequency-power comparison of GaN with other semiconductor contenders is shown in Figure 2.4. GaN covers a wider frequency spectrum and also maintains a higher RF output power as compared to others. It has a strong competition with SiC on the lower frequency side and with GaAs and InP on the higher frequency side.

The five key characteristics offered by GaN-based semiconductor are –

- Higher dielectric strength
- Higher operating temperature
- Higher switching speed
- Higher current density
- Lower ON-resistance

Figure 2.5 depicts all these above mentioned advantages of GaN.

Many experiments of the GaN based HEMTs (AlGaN/GaN, AlInN/GaN and AlN/GaN) have already confirmed that GaN technology is far superior to Silicon technology [21] in terms of output power and operating frequency.

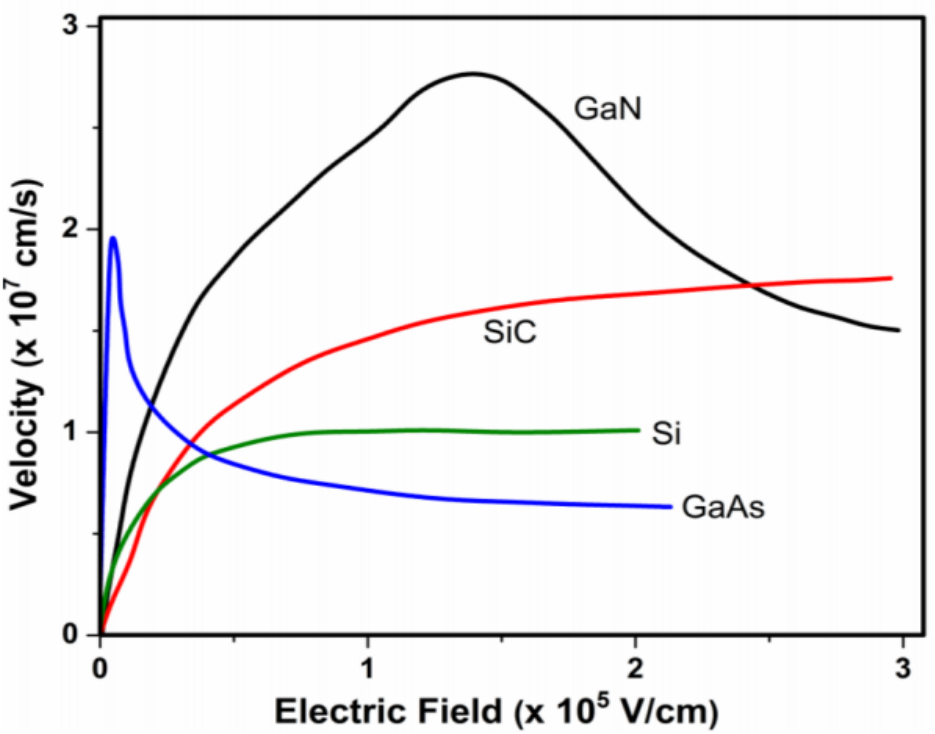


**Fig 2. 3 Saturation Velocity vs electric field characteristics of various semiconductors compared to GaN [18]**

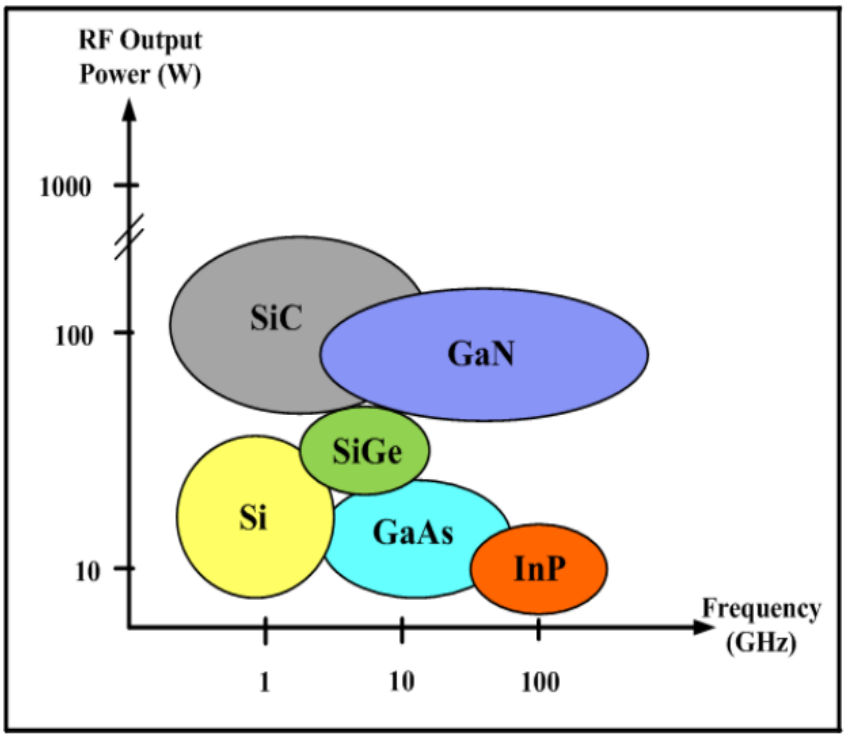


**Fig 2. 4 Semiconductor materials for RF applications. RF power is plotted against frequency [19]**

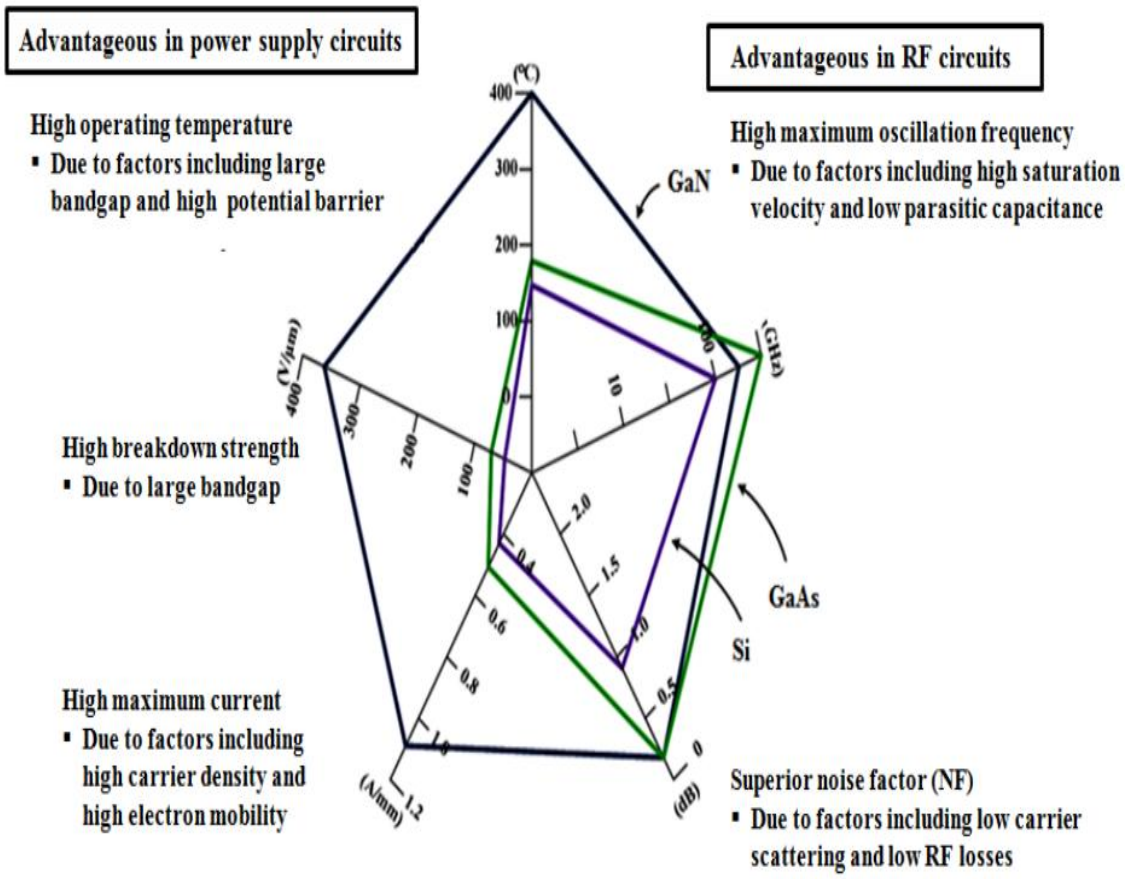


**Figure 2.5 GaN material merits compared to Si and GaAs [20]**

## 2.4 GaN Global Market

Currently, the overall GaN power semiconductors market accounts for less than 1% of the total power semiconductors market [22] ( currently at $34 billion including power discrete and power ICs), but over the next ten years, the entire base for power semiconductors and electronic players is expected to penetrate this new value chain, thereby rapidly increasing the percentage share.

At present GaN covers a wide range of application segments such as power distribution systems, heavy electrical systems, industrial systems, turbines, heavy

machinery, electro-mechanical computing systems, advanced industrial control systems, and so on. Another application segment is ICT, with several communication applications segments such as RF, satellite communication, RADAR offering huge revenue potential owing to the unbeatable ability of GaN to operate at operate at high frequency up to microwave range. These wide range applications of GaN make its total markets worth billions

The GaN market is quickly gaining high pace. Several diodes and transistors are available in the market since 2008. Within 6-7 years we can see extraordinary growth as now power discrete devices such as GaN based HEMT are ruling the power semiconductor market. Another factor for revenue growth is from GaN power ICs as several new power ICs such as MMICs and RFICs are launched in the market. Thereby the forecasted revenue for GaN power semiconductor is $1.75 billion by end of 2022[22].

The above discussed data is based on the extensive research study on GaN semiconductors market and industry which is aimed at identifying the entire market of the GaN semiconductor devices and its sub-segments that cover detailed classification taking in mind both revenue and shipment.

## 2.5 Polarization effect in AlGaN/GaN Heterostructure

In III-N semiconductors, there occurs a significant electrical polarization effects that dominate especially at the interfaces [23]. The polarization effects gains an importance similar or even greater than the impact caused by introducing doped impurity. Fig. 2.2 gives the crystal structure of wurtzite GaN. The reason for polarization in GaN is its non-

centrosymmetric structure. This non-centrosymmetric structure leads to a strong iconicity and a residual electrical polarity of the semiconductor. Fig 2.2 shows the planar nature of symmetry. Because of the polarization effect, GaN based HEMTs and MOS-HEMTs can be fabricated with heterostructure having no intentional or deliberate doping i.e. intrinsic layers. The polarization effect helps to clearly understand the concept of two Dimensional Electron Gas (2DEG) which will be discussed in the next section. The 2DEG density observed will have a strong dependence on the thickness and composition of AlGaN barrier layer in AlGaN/GaN HEMT.

***Basically there are two types of polarization introduced in GaN based heterostructure:***

- ***Spontaneous Polarization***
- ***Piezoelectric Polarization***

### 2.5.1 Spontaneous Polarization:

The spontaneous polarization occurs along the c-axis of the wurtzite structure and leads to a strong electric field of about 3MV/cm [24]. This type of polarization mainly depends on the polarity of the crystal structure. The terms spontaneous simply means zero strain thus it is polarization that occurs due to bonds between Cations (Ga) site and Anion (N) site being non-centrosymmetric along the c direction (0001) in a GaN crystal structure [25]. In this kind of polarization no external intervention takes place in the structure as hence crystal stays in equilibrium position [26]. Tetrahedral stick and ball diagram shown in fig. 2.6 explains the polarization vector present in the GaN crystal. The directions of the polarization in this structure are defined as such due to the electron

clouds being closer to the N atoms [26]. This difference in electronegativity together with the non –Centro symmetrical structure causes a polarization dipole to exist between Cation (Ga) site and Anion (N) site. Only the vertical component of spontaneous polarization in the three diagonal bonds has been considered and the horizontal component is assumed to be cancelled out.

The difference in polarization across a cross the interface of the two layers (AlGaN/GaN) will result in polarization charge to be present at the interface of the heterostructure. Difference in polarization may result because of difference in electronegativity across the hetero-interface that mainly depends on the composition of the adjacent layers in the heterostructure. In fig. 2.7, spontaneous polarization in GaN and AlGaN compound semiconductor is shown for [0001] growth direction. This direction is also called Ga-face polarity for GaN. Deviation from the lattice parameters also affects the magnitude of polarization. Equilibrium lattice parameters for wurtzite crystal structure parallel and perpendicular to growth direction are called $c_o$ and $a_o$. The $c_o/a_o$ ratio and the spontaneous polarization value of GaN and AlN is given in table 2.2. Variation in the $c_o/a_o$ ratio from the ideal value causes enhancement in spontaneous polarization.

| parameter | ideal | GaN | AlN |
|---|---|---|---|
| $c_0/a_0$ | 1.633 | 1.6266 | 1.6009 |
| $P_{SP}$, ($C/m^2$) | – | -0.029 | -0.081 |

**Table 2.2 $c_o/a_o$ value and spontaneous polarization value of wurtzite crytal GaN and AlN**

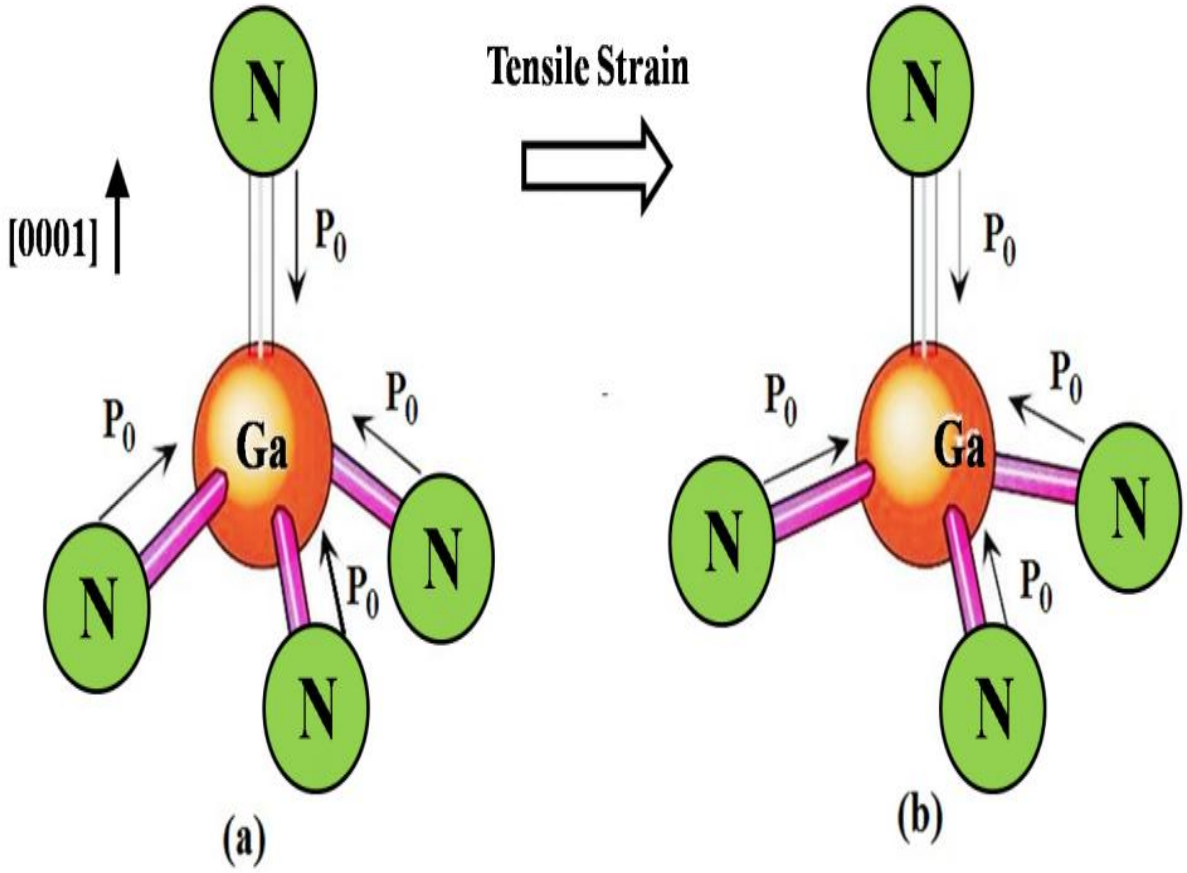


**Figure 2.6 Tetrahedral Stick and ball representation of GaN under (a) No Strain (b) Tensile Strain [27]**

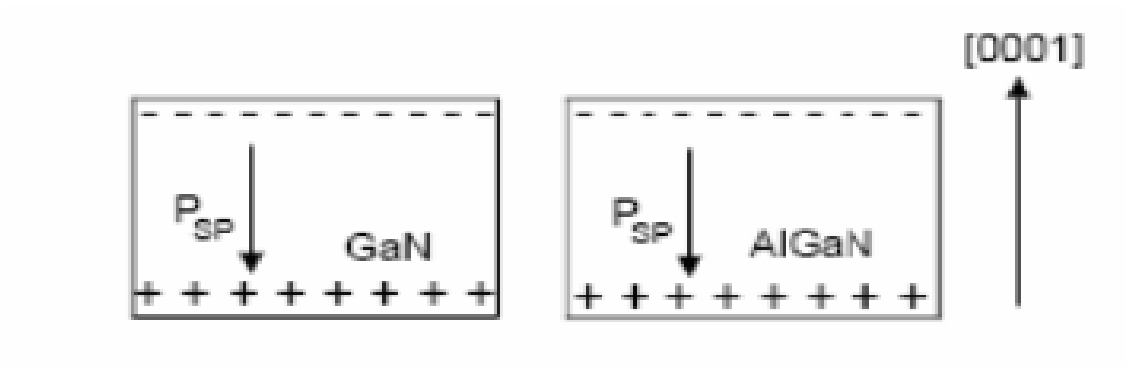


**Figure 2.7 Spontaneous Polarization fields and sheet charges occurred in GaN and AlGaN grown in [0001] direction.**

### 2.5.2 Piezoelectric Polarization:

In addition to the natural no ideality of the crystal lattice, external intervention have also effect on lattice parameters. Due to the lattice mismatch between the two materials strain is occurred at the heterostructure interface. This may even occur because of difference in thermal coefficient of expansion between the adjacent layers. Thus may result into either a compressive stress or a tensile one [28]. Consequently axial stress takes place on the plane of intersection. This stress is absorbed via the change in the lattice parameters $a_o$ and $c_o$ of the crystal structure. Quite similar to the spontaneous polarization case new equillibrium state causes alternation in polarization strength in the materials. This type of polarization is called Piezoelectric Polarization.

Let us consider wurtzite AlGaN/GaN heterostructure grown in [0001] direction. Since lattice parameters of AlGaN compound are slightly smaller than those of GaN, AlGaN layer is under tensile stress and inversely GaN layer is under compressive stress. The tensile stree of AlGaN decreases $c_o/a_o$ ratio and therefore generates a piezoelectric polarization in AlGaN layer which has same direction with the spontaneous polarization as shown in figure 2.8. For the case of thick enough GaN layer, the compressive stress is relaxed and absorbed by the whole GaN structure. As a result, no piezoelectric effects are observed in GaN buffer.

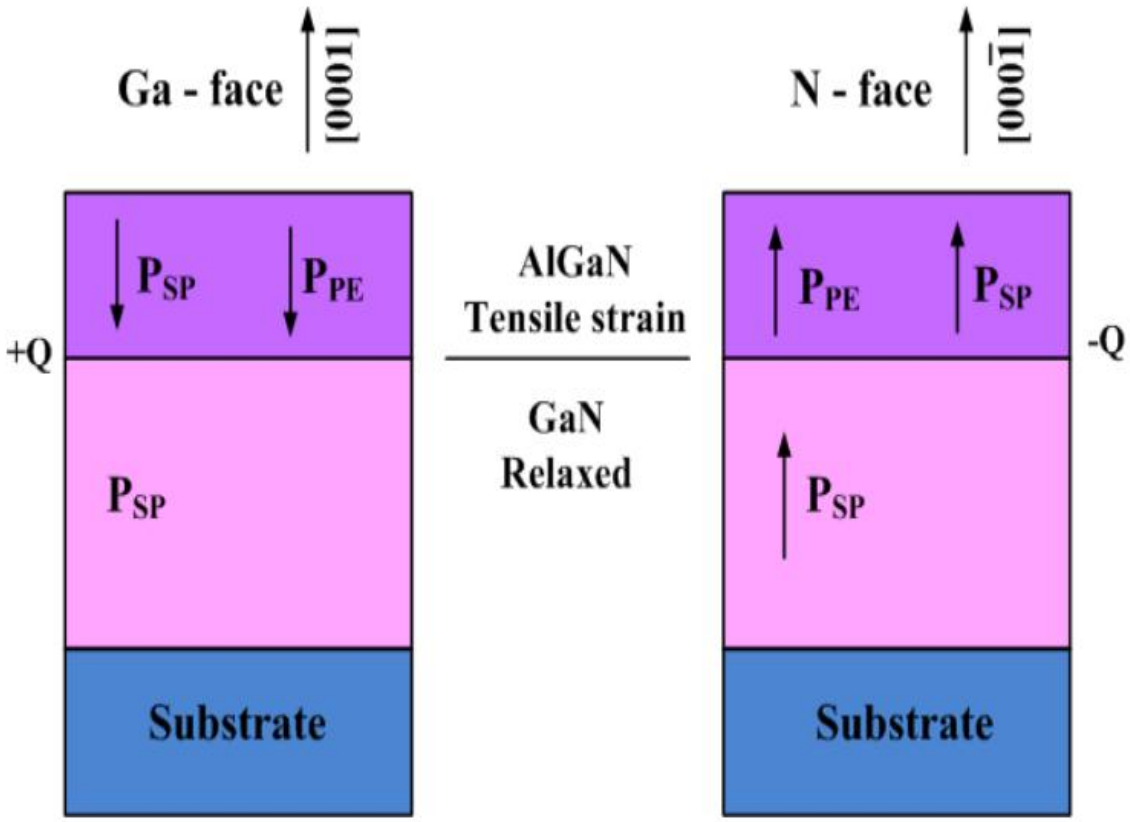


**Figure 2.8 The AlGaN/GaN heterostructure with polarization induced sheet charge density and the direction of the spontaneous and piezoelectric polarization in Ga- and N-face.**

In contrast with the spontaneous polarization, where the polarization depends on the alloy type and composition of the alloy, the piezoelectric polarization requires additional information such as strain, piezoelectric coefficients and elastic constants, all of which might be directly or indirectly affected by the composition of nitride alloys. The resultant polarization (combined effect of spontaneous and piezoelectric) induced sheet charge density and the directions of both types of polarization in the AlGaN/GaN heterostructure.

Owing to surface donor-like traps [29], piezoelectric polarization brings the concept of 2DEG which is basically a sheet of electrons at the GaN side of the interface which has been discussed in the next section.

## 2.6 Concept of 2DEG

Suppose there is no external electric field applied on the AlGaN/GaN heterostructure. The total polarization (P) of the system is represented by the addition of spontaneous polarization ($P_{SP}$) and piezoelectric polarization ($P_{PE}$). Since all polarization vectors are directed to z-axis in this case. For AlGaN/GaN the total macroscopic polarization is given by –

$$\mathbf{P = P_{SP} + P_{PE}} \qquad \mathbf{(2.1)}$$

As we have already discussed thick GaN layer contains only spontaneous polarization. Discontinuity of polarization at the interface causes a bound sheet charge density ($\boldsymbol{\sigma_p}$) as per Gauss law :

$$\boldsymbol{\sigma_p = P_{PE,AlGaN} + P_{SP,AlGaN} - P_{SP,\,GaN}} \qquad \mathbf{(2.2)}$$

Piezoelectric polarization is given by :

$$\mathbf{P_{PE} = e_{33}\,\varepsilon_x + e_{31}\,(\varepsilon_x + \varepsilon_y)} \qquad \mathbf{(2.3)}$$

where $e_{33}$ and $e_{31}$ are piezoelectric constants. $e_{33}$ is in z-direction and $e_{31}$ is in x and y direction respectively.

The piezoelectric polarization in AlGaN layer can be expressed as:

$$P_{\mathrm{PE}} = 2\frac{a-a_0}{a_0}\left(e_{31} - e_{33}\frac{C_{13}}{C_{33}}\right). \qquad \mathbf{(2.4)}$$

Combining equation (2.2) and (2.4) the polarization induced sheet charge density $\boldsymbol{\sigma_p}$

At AlGaN/GaN interface is given by:

$$|\sigma_P| = \left| 2\frac{a-a_0}{a_0}\left\{ e_{31} - e_{33}\frac{C_{13}}{C_{33}} \right\} + P_{\mathrm{SP,AlGaN}} - P_{\mathrm{SP,GaN}} \right| . \qquad \textbf{(2.5)}$$

Calculation of above equation confirms that the sheet charge density increases with the increment of Al composition rate of AlGaN [30]. Equation 2.5 shows AlGaN/GaN heterostructure generates 10 times higher sheet charge density compared to other counterparts [31]. So it is a powerful candidate for HEMT.

In addition to polarization concept, band offset at conduction band makes AlGaN/GaN heterostructure special for high current and high power microwave applications. Beyond a critical thickness of undoped AlGaN layer, discontinuity at the conduction band forces energy level to fall below the Fermi level and results into a triangular-like quantum well at the AlGaN/GaN heterojunction interface as shown in the figure 2.9.

Beyond a critical thickness of AlGaN layer polarization fields become high enough to ionize surface donors states. These ionized electrons move towards the AlGaN/GaN interface under the effect of internal electric fields and fill the triangular well-formed just like a quantum well. This negative charge assembled at the interface called ***two dimensional electron gas, 2DEG***. Accordingly, the ionized surface donor states form a positive charge $\sigma_{comp}$ at the surface of AlGaN layer as shown in figure 2.9,

which compensates the negative sheet charge $\sigma_{surf}$ generated due to polarization induced sheet charge $\sigma_{p.}$

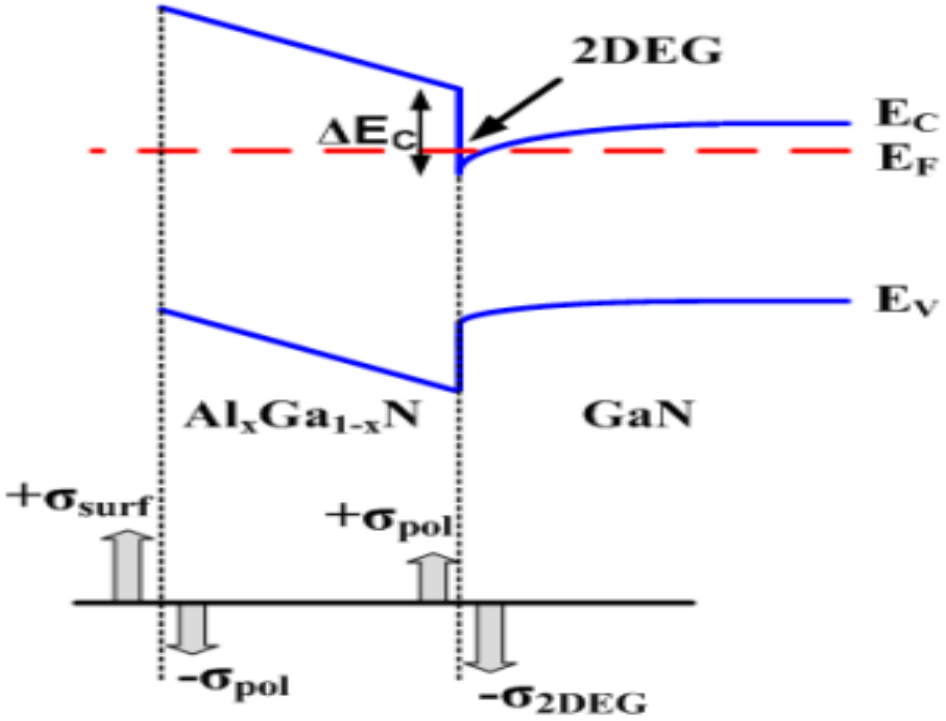


**Fig. 2.9 Energy band diagram of AlGaN/GaN heterostructure showing quantum well, and charge density at the AlGaN/GaN interface and AlGaN surface.**

The most accurate and consistent model for 2DEG formation is the surface donor model [32] according to which surface donors are the source of electrons in the 2DEG channel as we explained before. Formation of 2DEG and the effect of critical thickness is shown in figure 2.10.

It is clear from Fig 2.10 (a) that no 2DEG formation is observed up to the critical thickness of AlGaN layer. On the other hand, 2DEG formation occurs for AlGaN layer

thickness higher than $d_{cr}$ that is shown in figure 2.10(b). Conductivity of the 2DEG channel formed is a crucial parameter for HEMT operation, which mainly depends on the sheet carrier concentration and mobility of the electron in the channel.

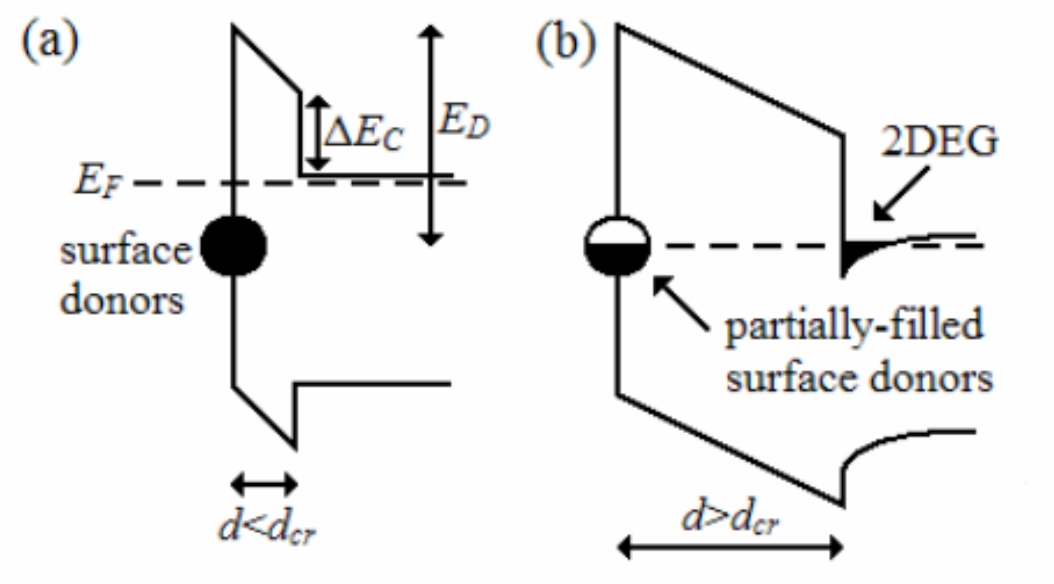


**Fig. 2.10 Illustration of Surface Donor Model [32]**

Surface quality of the HEMT structure is an important parameter since 2DEG characteristics is based on surface-donor like states, which constitutes the core of HEMT operation. Surface can be affected for various external and internal factors.

## 2.7 DEVICE STRUCTURE AND SIMULATION METHODOLOGY

### 2.7.1 INTRODUCTION

This section will describe simulations which have been carried out relevant to this research. Device simulation and modelling are crucial in the development of any

technology allowing designers to optimize device designs and process flows before putting them into production. This is particularly true for GaN based devices when considering the large cost of the material. Some initial attention will focus on a description of the software and other aspects of the device operation.

Software based simulations approach can be effectively used to tailor the device structure for explicit market application demanding particular set of performance characteristics as it provides deeper insights into device physics and its operation, helps in optimizing the device structural parameters, and helps to understand the degradation mechanisms associated with scaling of devices. The process and device simulation tools are collectively termed as TCAD (Technology Computer Aided Design). With the rapid advancement of the IC industry, technology computer aided design (TCAD) has undergone a continuous evolution. The TCAD tools can be used to design, develop and optimize a wide range of existing and upcoming technologies ranging from highly scaled CMOS, power management, optoelectronics, non-volatile memory, image sensors, solar cells, and analog/RF devices. Synopsys TCAD contains a complete suite of products that includes tools for process and device simulation. Device simulation tools simulate the electrical characteristics of devices, in response to external electrical stimulus, and other thermal or optical boundary conditions imposed [33].

Here, we have used the Sentaurus Device tool for our simulation. Sentaurus Device is a 2D/3D device simulation tool capable of simulating silicon-based

and compound semiconductor based devices. It simulates advanced quantization models including rigorous Schrödinger solution and complex tunneling mechanisms for transport of carriers in heterostructure devices like HEMTs, MOS-HEMTs and HBTs made from GaAs, InP, GaN, SiGe, SiC, AlGaAs, InGaAs, AlInN, AlGaN and InGaN.

In this section we also elucidate the device structure of the novel InAlN/AlN/GaN based Gate Recessed HEMT. The structural details such as layer thicknesses, lengths, widths, doping profiles, trap concentrations, etc. are given. The key material parameters of the device are elaborated. The polarization charge considered at each interface is then listed. The calibration of the simulation model is done with the experimental results. The models used for accounting the physical effects associated in the device are also explained.

## 2.7.2 DEVICE STRUCTURE

The 2D device layout of the InAlN/AlN/GaN based Gate Recessed HEMT used in the simulation is shown in Fig. 3.1. The device has gate length (Lg) of 100 nm. Here we introduced T-gate in the already proposed n++ GaN/InAlN/AlN/GaN HEMT [34]. GaN buffer and AlN thickness are considered to be 2µm and 1 nm respectively. Thickness of lattice matched $In_{0.17}Al_{0.83}N$ barrier and GaN Cap is maintained at 1 nm and 6 nm respectively. The source-to-gate spacing is 1 µm and that of gate-to-drain is 2.9 µm. The cap doping density is 2E20 cm-3 and that of lattice matched $Al_{0.83}In_{0.17}N$ barrier layer doping density is 5E16 cm-3. The AlInN barrier layer has a wide conduction band edge offset with GaN and is nearly lattice matched, to minimize the strain related defects. The

barrier layer provides a strong carrier confinement in the quantum well at the hetero-interface.

To enhance the quantum well electron mobility the best proposal would be to introduce channel-to-gate separation of 2 nm that consists of 1 nm InAlN barrier layer and 1 nm AlN spacer layer respectively. In our proposed device there is no direct contact between the n++ GaN cap layer and gate. Both thickness and high doping of the GaN cap layer influences HEMT direct current and microwave performance. Unintentional n-type doping is compensated by additionally added p-type doping i.e. Fe-doping or C-doping. The resist for etching the GaN cap under the gate electrode is undercut.

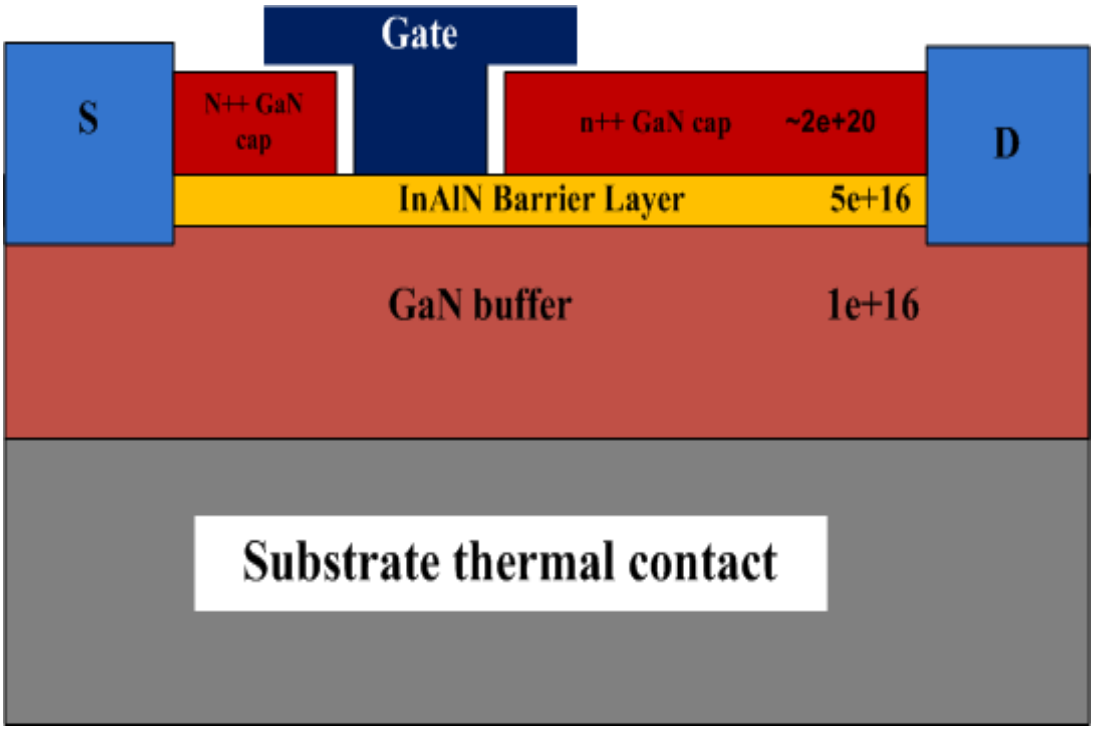


**Fig. 2.11 Cross-sectional view of T-gate E-mode n++GaN/InAlN/AlN/GaN high electron mobility transistor.**

## 2.7.3 MATERIAL PARAMETERS

Some discrepancies are observed between theoretically calculated GaN material parameters and those that are experimentally measured. Thus, the main material parameters for GaN and AlInN used in the current simulations are listed in Table 3.1. The Al0.83In0.17N is lattice matched to GaN and the heterostructure is stacked along the c-axis. As Al0.83In0.17N and GaN are lattice matched there is no strain in the heterostructure. The absence of stain results in only spontaneous polarization.

It is clear from the structure that the sum of total negative charge of InAlN/AlN interface and total positive polarization charge at AlN/GaN interface is contributing to total polarization charge. Polarization charge at the two interfacing surface is assumed to be fixed and is given by $\sigma_{InAlN/GaN} = 2.7\times10^{13}$ and $\sigma_{InAlN/n++GaN} = -2.7\times10^{13}$ respectively.

| Material | GaN | $Al_{0.83}In_{0.17}N$ |
|---|---|---|
| $E_g$(eV) | 3.4 | 4.7 |
| CBO (eV) | 0.57 | - |
| VBO (eV) | 0.73 | - |
| $\varepsilon_0$ | 9.5 | 11.7 |
| Lattice Constant (A) | 3.186 | 3.190 |
| $\mu_e$(cm²/Vs) | 940 | 1540 |
| $\mu_e$(cm²/Vs) | 22 | 82 |

**Table 2.3 Physical Properties of Al0.83In0.17N and GaN.**

### 2.7.4 SIMULATION FRAMEWORK

In this section, we explain the 2D simulation of InAlN/AlN/GaN based Gate Recessed HEMT performed with Sentaurus Device simulator [35]. Depending on the device under investigation and the level of accuracy required, the user can select the transport model. Sentaurus TCAD provides drift diffusion, thermodynamic, hydrodynamic models for simulating the device transport. The drift diffusion (DD) model assumes that the carriers are in thermal equilibrium with the lattice. Whereas, the hydrodynamic (HD) model assumes that the electron and hole temperatures are not equal to the lattice temperature. Thus HD model involves more complex current density expressions than compared to DD model as they carrier temperature gradients into consideration. The HD model accurately considers the non- equilibrium conditions such as quasi-ballistic transport in the thin regions and the velocity overshoot effect in the depleted regions. Several important physical effects such as bandgap narrowing, variable effective mass and doping dependent mobility at high electric fields are also accounted in HD simulations.

In high speed devices electrons may attain very high speed, leading to non-equilibrium transport. Thus the electron velocity can be much greater than the steady state velocity. DD simulations cannot accurately model this non-equilibrium electron transport occurring in the hetero-structures devices. The Monte Carlo method can perform accurate simulation by solving the Boltzmann's transport equations, but are time consuming and tedious. Therefore, we have preferred HD model to simulate and analyze device performance of the proposed InAlN/AlN/GaN based Gate Recessed HEMT. Charge

balance at the interface has been taken into consideration in case of ohmic contact. Ideal Neumann condition i.e. the screening method is used at the interface without contact. The thermal contact is characterized by thermal resistance values.

Charge balance at the interface has been taken into consideration in case of ohmic contact. Ideal Neumann condition i.e. the screening method is used at the interface without contact. The thermal contact is characterized by thermal resistance values.

The Thermodynamic model utilized can be solved by using the Poisson and Continuity equations as given below:

$$\nabla \cdot \varepsilon \nabla \phi = -q(p - n + N_D - N_A) - \rho_{trap.} \quad \textbf{(3.1)}$$

$$J_n = -nq\mu_n(\nabla \Phi_n + P_n \nabla T) \quad \textbf{(3.2)}$$

where **ε** is the electrical permittivity, **ϕ** is the electrostatic potential, **q** is the electronic charge, **n** and **p** are electron and hole densities, $\mathbf{N_D}$ is the concentration of ionized donors, $\mathbf{N_A}$ is the concentration of ionized acceptors and $\rho_{trap}$ is the charge density contributed by traps and fixed charges, $\boldsymbol{\phi_n}$ is the Fermi quasi potential, $\mathbf{P_n}$ is the absolute thermoelectric power, and **T** is the lattice temperature.

The doping and field dependent mobility model has been considered while undergoing simulations. The doping-dependent mobility is modeled after Arora and can be given by following equations:

$$\mu_{n,dop} = \mu_{min} + \frac{\mu_d}{1 + ((N_{A,O} + N_{D,O}) / N_0))^{A*}} \quad \textbf{(3.3)}$$

$$\mu_{min} = A_{min}\,(T/300)^{\alpha}{}_{m} \quad \textbf{(3.4)}$$

$$\mu_{d} = A_{d}\,(T/300)^{\alpha}{}_{d} \quad \textbf{(3.5)}$$

$$N_{o} = A_{N}\,(T/300)^{\alpha N} \quad \textbf{(3.6)}$$

$$\mu_{*} = A_{\alpha}\,(T/300)^{\alpha\alpha} \quad \textbf{(3.7)}$$

Where $\boldsymbol{\mu_{min}}$**,** $\boldsymbol{\mu_{d}}$**, N0, and A*** are temperature dependent coefficients taken from [36]. Parameters values of $\boldsymbol{v_{sat}}$ **= 1.3 x 10$^{7}$ cm/s** and $\boldsymbol{\mu_{min}}$ **= 800 cm$^{2}$/V-s** are used in the simulation.

High field mobility is governed by following equation:

$$\mu(E) = \frac{\mu_{low} E}{\left[1 + \left(\frac{\mu_{low} E}{v_{sat}}\right)^{\beta}\right]^{\frac{1}{\beta}}} \quad \textbf{(3.8)}$$

In our simulation SRH model has been introduced that accounts for the recombination effect in the bandgap.

$$R_{SRH} = \frac{np - n^{2}_{ie}}{\left[\tau_{p}(n + n_{1}) + \tau_{n}(p + p_{1})\right]} \quad \textbf{(3.9)}$$

where, $\boldsymbol{\tau_{n}}$ and $\boldsymbol{\tau_{p}}$ denote the temperature dependent lifetime of electrons and holes, respectively and $\boldsymbol{n_{ie}}$ is the effective intrinsic density. Additional auxiliary concentrations $\boldsymbol{n_{1}}$ and $\boldsymbol{p_{1}}$ coming from the deep levels are modeled by:

$$n_{1} = n_{ie} e \frac{E_{trap}}{kT} \quad \textbf{(3.10)}$$

$$p_{1} = p_{ie} e \frac{E_{trap}}{kT} \quad \textbf{(3.11)}$$

Where, $\boldsymbol{E_{trap}}$ is the difference between the intrinsic level and the defect level.

The parameters necessary to compute **$\mu_d$, N0, and A*** are listed in Table3.2.

As the model is analysed, we will now determine transfer characteristics, transconductance, leakage current, transconductance generation factor, $f_T$, $f_{max}$ of the said device.

| Parameter | Value |
|---|---|
| $A_{min}$ ($cm^2V^{-1}s^{-1}$) | 75.9322 |
| $\alpha_m$ | 2.1894 |
| $A_d$($cm^2V^{-1}s^{-1}$) | 5204.361 |
| $\alpha_d$ | -3.2933 |
| $A_N$($cm^{-3}$) | 2E+17 |
| $\alpha_N$ | 7.365 |
| $A_a$ | 0.40252 |
| $\alpha_a$ | -0.20567 |

**Table 2.4 Parameters necessary to compute the temperature and doping dependent electron mobility of Al0.83In0.17N.**

## Summary:

The chapter starts with the physical aspect of III-V compound semiconductors and then compares several III-V group materials and bring out there positive aspect over Si and Ge. The chapter further includes the material and structural properties of GaN and unique properties of GaN based devices. The chapter covers detailed explanation of the

concept of polarization and then what leads to the formation of 2DEG. The factors effecting the 2DEG formation and sheet charge density. The crucial parameters for HEMT operation are explained. The chapter further discuss device structure and simulation framework of InAlN/AlN/GaN based Gate Recessed HEMT. The material parameters of Al0.83In0.17N and GaN used in the simulation, along with the polarization charges at each interface are also explained. The fundamental models used in the simulation work are explained. We will now determine transfer characteristics, transconductance, leakage current, transconductance generation factor, $f_T$, $f_{max}$ of the said device in the next section.

## REFERENCES

[1] 2.122. S. Fu, Y. Chen, Appl. Phys. Lett. **85** 1523 (2004)

[2] A. Shanware, J. McPherson, M. Visokay, J. Chambers, A. Rotondaro, H. Bu, M. Bevan, R. Khamankar, L. Colombo, in *IEDM Technical Digest*, Washington DC, 2001, pp. 137–140

[3] E. Gusev et al., in *IEDM Technical Digest*, San Francisco, 2004, pp. 79–82

[4] C. Hobbs, Leonardo, R. Fonseca, A. Knizhnik, V. Dhandapani, S. Samavedam, W. Taylor, J. Grant, L. Dip, D. Triyoso, R. Hegde, D. Gilmer, R. Garcia, D. Roan, M. Lovejoy, R. Rai, E. Hebert, H. Tseng, S. Anderson, B. White, P. Tobin, IEEE Trans. Electron Devices **51**, 971 (2004)

[5] J. Edgar, in *Properties of Group III Nitrides*, No. 11 in EMIS Data reviews Series, ed. by J. Edgar (IEE INSPEC, London, 1994), Sect. 1.2, pp. 7–21

[6] A. Chakraborty, B. Haskell, S. Keller, J. Speck, S. Denbaars, S. Nakamura, U. Mishra, Jpn. J. Appl. Phys. **44**, L173 (2005)

[7] K. Okamoto, H. Ohta, S. Chichibu, J. Ichihara, H. Takasu, Jpn. J. Appl. Phys. **46**, L187 (2007)

[8] O. Ambacher, ”Growth and applications of Group III-nitrides”, *Journal of Physics D: Applied Physics*, Vol. 31, No. 20, 1998.

[9] O. Ambacher *et al.*, “Two-dimensional electron gases induced by spontaneous and piezoelectric polarization charges in N- and Ga-face AlGaN/GaN heterostructures”, *J. Appl. Phys.*, Vol. 85, No. 6, 1999.

[10] F. Bernardini, ”Spontaneous and Piezoelectric Polarization: Basic Theory vs. Practical Recipes”, *Nitride Semiconductor Devices: Principles and Simulation*, J. Piprek, Ed.: Wiley-VCH Verlag GmbH and Co., 2007.

[11] T.P.Chow and R.Tyagi, “Wide bandgap compound semiconductors for superior high-voltage unipolar power devices,” IEEE Trans. On El. Devices., Vol.41, No. 8, pp. 1481-1483.Aug, 1994.

[12] H. Morkoc, S. Strite, G. B. Gao, M. E. Lin, B. Sverdlov, and M. Burns, “Large-band-gap SIC, III-V nitride, and II-VI ZnSe-based semiconductor device technologies,” J. Appl. Phys., Vol.76, No. 3, 1 August 1994.

[13] Binari, S.C., Rowland, L.B., Kruppa, W., Kelner, G., Doverspike, K. and Gaskill, D.K., 1994. Microwave performance of GaN MESFETS. *Electronics letters*, *30*(15), pp.1248-1249.

[14] Trivedi, Malay, and Krishna Shenai. "Performance evaluation of high-power wide band-gap semiconductor rectifiers." *Journal of Applied Physics* 85.9 (1999): 6889-6897.

[15] Ionascut-Nedelcescu, A., et al. "Radiation hardness of gallium nitride."*Nuclear Science, IEEE Transactions on* 49.6 (2002): 2733-2738.

[16] Mistele, David. *Technology of AlGaN/GaN Heterostructure MOSHFETs*. Mensch-und-Buch-Verlag, 2003.

[17] U. K. Mishra *et al.*, “AlGaN/GaN HEMTs—Overview of device operation and applications”, *Proceedings of the IEEE*, Vol. 90, No. 6, 2002.

[18] R. J. Trew, “SiC and GaN Transistors—Is there one winner for microwave power applications?”, *Proceedings of the IEEE*, Vol. 90, No. 6, 2002.

[19] Yole Development, Wide Report: “World Market for wide bandgap materials and devices for RF applications,” *Global Informatics, Inc*, 2005.

[20] http://techon.nikkeibp.co.jp/

[21] W. Nagy, J. Brown, R. Borges, and S. Singhal. "Linearity characteristics of microwave-power GaN HEMTs," *IEEE Transactions on Microwave theory and Techniques*, Vol.51, no. 2, pp. 660-664, 2003

[22] http://www.marketsandmarkets.com/PressReleases/gallium-nitride semiconductor.asp

[23] C. Wood, D. Jena (eds.), *Polarization Effects in Semiconductors* (Springer, New York, 2008)

[24] O. Ambacher, J. Smart, J. Shealy, N. Weimann, K. Chu, M. Murphy, R. Dimitrov, L. Wittmer, M. Stutzmann, W. Rieger, J. Hilsenbeck, J. Appl. Phys. **85**, 3222 (1999)

[25] H. Morkoc, R. Cingolani, B. Gil, "Polarization effects in Nitride Semiconductor Device Structures and Performance of Modulation Doped Field Effect Transistors," Solid-State Electronics, vol. 43, no.10, pp. 1909-1927, 1999.

[26] F. Bernardini, V. Fiorentini, and D. Vanderbilt, "Spontaneous Polarization and piezoelectric constants of III-V nitrides," Phys. Rev. B, Vol. 56, No. 16, Oct. 1997.

[27] C. Wood, Polarization Effects in Semiconductors, Springer Verlag, pp. 380-383, 2008.

[28] Low Kim Fong Edwin, "Characterization and Numerical Simulation of Gallium Nitride-based Metal-Oxide-Semiconductor High Electron Mobility Transistor with high-k gate stack," Ph.D Thesis, *National University of Singapore*, 2011.

[29] Smorchkova, I. P., et al. "Polarization-induced charge and electron mobility in AlGaN/GaN heterostructures grown by plasma-assisted molecular-beam epitaxy." *Journal of applied physics* 86.8 (1999): 4520-4526.

[30] Kramer, Mark Cornelia Johannes Carolus Maria. "Gallium nitride-based microwave high-power heterostructure field-effect transistors: design, technology, and characterization." *Dissertation Abstracts International* 68.02 (2006).

[31] W.Q.Chen and S.K.Hark, *J. Appl. Phys*., 77,5747,1995

[32] Ibbetson, J. P., et al. "Polarization effects, surface states, and the source of electrons in AlGaN/GaN heterostructure field effect transistors." *Applied Physics Letters* 77.2 (2000): 250-252.

[33] http://www.synopsys.com/Tools/TCAD/Pages/default.aspx

[34] J. Kuzmík, C. Ostermaier, G. Pozzovio, B. Basnar, W. Schrenk, J.-F. Carlin, M. Gonschorek, E. Feltin, N. Grandjean, Y. Douvry, Ch. Gaquière, J.-C. De Jaeger, K. Ci ˇ co, ˇ K. Fröhlich, J. Skriniarová, ˇ J. Kovác, ˇ G. Strasser, D. Pogany, E. Gornik, Proposal and performance analysis of normally off n++ GaN/InAlN/AlN/GaN HEMTs with 1-nm-thick InAlN barrier, IEEE Trans. Electron Dev. 57 (September (9)) (2010) 2144-2154.

[35] Synopsys. TCAD Sentaurus Software VG-2012.06.1

[36] TCAD Sentaurus, SDevice User Guide, ver. G-2012.06, Synopsys, 2012 June.

# *Chapter 3*

# PERFORMANCE ANALYSIS FOR VARYING DRAIN VOLTAGE AND $n^{++}$ GaN CAP DENSITY

## 3.1 INTRODUCTION

In order to achieve improved high frequency operation the gate length of existing InAlN/GaN HEMT needs to be scaled down. T-gate structure is a solution to achieve the desired high frequency performance. T-gate enhancement mode AlInN/GaN HEMT are also seen in the literature [1-3] and have resulted in improved RF performance. However, in all the structures discussed so far T-gate is recessed through the top barrier layer which leads to major Short Channel Effect (SCE) restrictions on high frequency performance [4]. S. Adak et al. reported a $f_t$ of 123GHz for the 150nm T-gate recess enhancement mode AlInN/GaN HEMT having less SCE by using p-GaN back barrier concept but drain current is reduced which is a drawback of that device [5].

In 2013, D.M. Geum et al. presented $f_T$ = 170 GHz in a 75nm T-gate AlInN/GaN HEMT [6] and in the same year L. Bo et al. demonstrated a 200nm T-gate AlInN/GaN HEMT having $f_t$ of 60 GHz [7], both the device reduced SCE due to the insertion of AlGaN back barrier but these two devices are in depletion mode HEMT which is hard to use for switching application.

In this work, we proposed a novel device structure having T-gate $n^{++}$GaN/InAlN/AlN/GaN HEMT which support enhancement mode but T-gate is not recessed through AlInN top barrier layer which ensures low SCE, high drain current, and higher cut off frequency, $f_T$. The performance of the said device needs to be investigated systematically for the inspection of its capability for high frequency as well

as switching applications. Hence, we have performed the simulations comprehensively to determine the various characteristics of the device accurately.

This chapter compares various DC and RF parameters of the proposed device such as transconductance, leakage current, transconductance generation factor, $f_T$, $f_{max}$ for varying drain voltage from 3V to 5V. To the best of our knowledge, a detailed analysis of the effect of varying drain voltage on the device performance of T-gate $n^{++}$GaN/InAlN/AlN/GaN HEMT is not done yet. Thus, we have comprehensively analyzed the impact of Drain voltage on device performance of T-gate $n^{++}$GaN/InAlN/AlN/GaN HEMT.

## 3.2 EFFECT OF DRAIN VOLTAGE VARIATION

### 3.2.1 DRAIN CURRENT ANALYSIS

Typical transfer characteristics of proposed 100nm T-gate $n^{++}$ GaN/InAlN/ AlN/GaN Enhancement mode HEMT but with three different drain bias voltages have been plotted in Figure 3.1. As the applied drain to source voltage increases there occurs a considerable negative shift in threshold voltage. A maximum drain current of 0.34A/mm is obtained at Vgs=1.2V for the drain bias of 5V by virtue of high mobility and velocity of 2DEG in the buried channel. High value of 2DEG density in the buried channel results in high drain current. As $V_{ds}$ increases, the barrier in the channel decreases, enhancing the electron injection from the source into the channel, leading to a significant increase of the drain current. For lower bias, the drain current is proportional to conductivity of the channel and for higher bias, the drain current is

proportional to carrier density and carrier injection velocity [8]. Maximum drain current plays an important role in a HEMT device when the device has to be utilized as power amplifier [9].

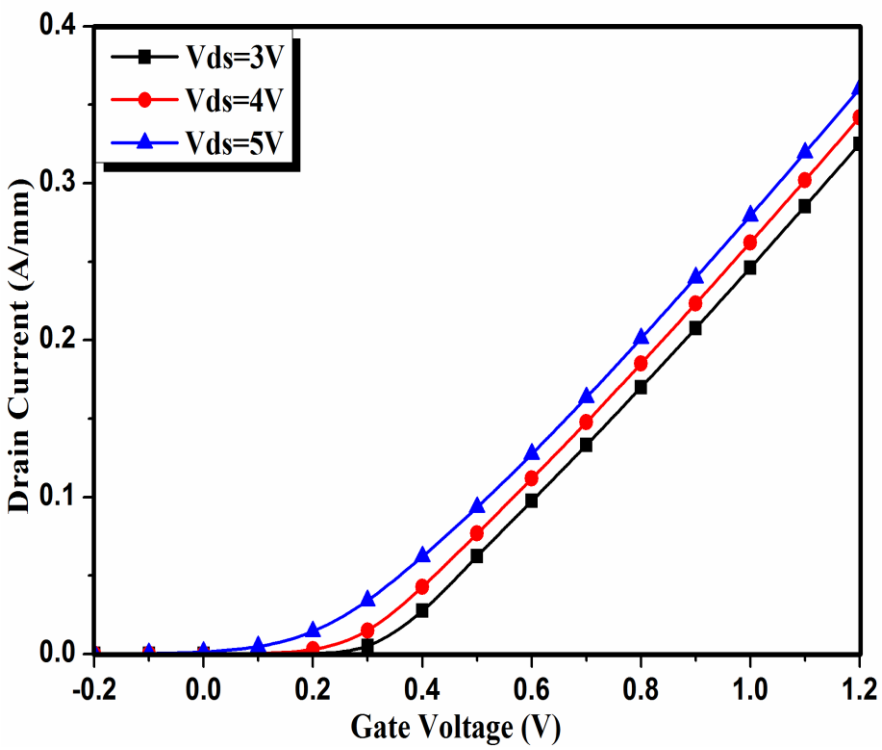


**Fig. 3.1 Simulated Transfer characteristics of T-gate $n^{++}$GaN/InAlN/AlN/GaN Enhancement mode HEMT, $L_g$=100nm.**

## 3.2.2 TRANSCONDUCTANCE VARIATION

Transconductance (for transfer conductance), also infrequently called as mutual conductance, is the electrical characteristic relating the current through the output of a device to the voltage across the input of a device. Transconductance can be obtained from the ratio of variation in $I_d$ to the variation of gate voltage ($V_{gs}$), for constant drain voltage

($V_{ds}$) [10]. The increase in current (and therefore $g_m$) can be evaluated as a function of the charge ($n$) and the velocity ($v$) increments. For CMOS applications a very high value of transconductance is acceptable. Because of polarization effect a very minute variation is observed in transconductance peak for varying drain bias.

Figure 3.2 represents transconductance variation with $V_{gs}$ for the proposed device. Here, it is observed that at a gate voltage of 1.2V a peak transconductance of 407.5 mS/mm is achieved at a drain bias of 5V. Broader $g_m$ profile provides an improved linear behavior from which a smaller intermodulation distortion, a smaller phase noise and a larger dynamic range could be expected [11].

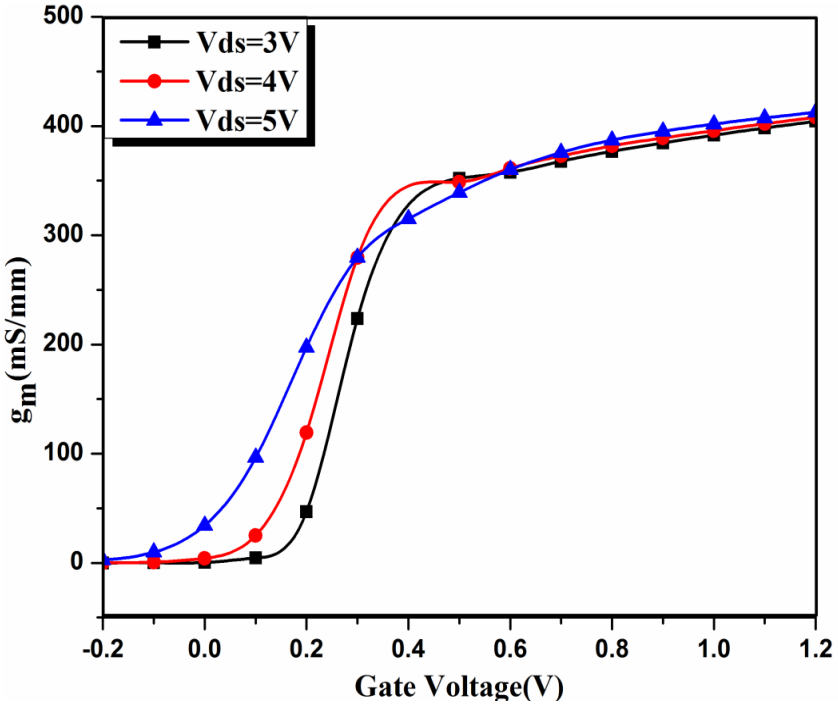


**Fig. 3.2 Simulated transconductance curve of T-gate $n^{++}$GaN/InAlN/AlN/GaN Enhancement mode HEMT.**

### 3.2.3 TRANSCONDUCTANCE GENERATION FACTOR

Transconductance-to-current ratio ($g_m/I_d$) also known as the transconductance generation factor (TGF) is a key figure of merit in the design of subthreshold low-power analog applications [11]. TGF can be defined as the available gain per unit value of power dissipation, because $g_m$ represents the gain, and $I_d$ represents the power dissipated to obtain that amplification. Lower TGF implies decreased input drive ability and hence, higher power dissipation in capacitive load circuits. TGF as a function of variable drain voltage is shown in figure 3.3. A very high value of 94.01 $V^{-1}$ is obtained at drain bias of 5V. This high value of TGF achieved is utilized in analog applications. TGF attains peak value at low gate bias and degrades severely at higher gate bias, due to increased value of $I_d$ at higher $V_{gs}$ .

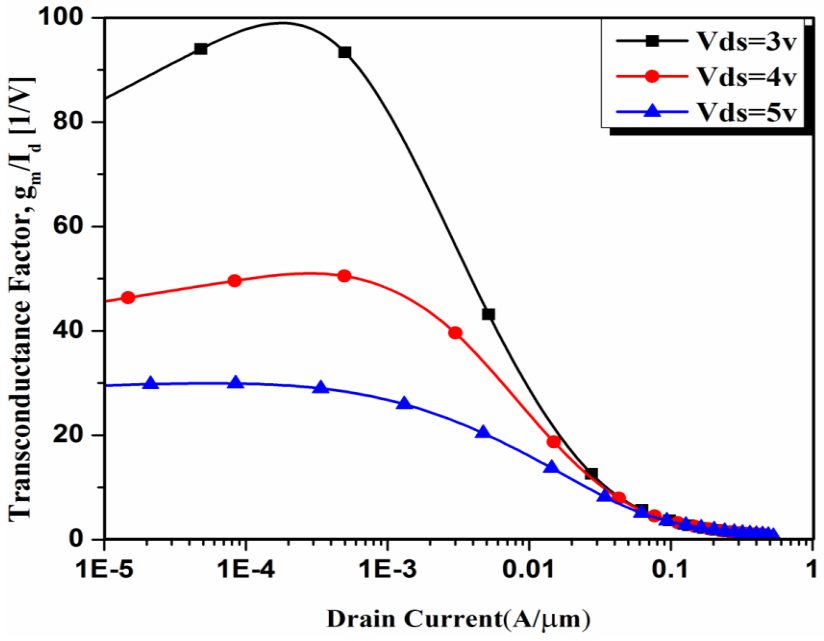


**Fig. 3.3 Dependence of Transconductance generation factor ($g_m/I_d$) on Drain Current.**

### 3.2.4 GATE LEAKAGE CURRENT

As the continuous down-scaling of the device size has led to very thin gate oxides, the leakage current that can flow from the channel to the gate comes into the order of the subthreshold leakage current and the gate cannot be considered as an ideally insulated electrode anymore. This affects the circuit functionality and increases the standby power consumption due to the static gate current. Even though we are simulating our device at room temperature, Poole-Frenkel emission component has been only considered for gate leakage current. Gate leakage current vs. gate voltage has been plotted in Figure 3.4 for the proposed device and is in the order of $10^{-5}$ as observed from the plot which is very low due to introduction of T-Gate. Low gate leakage current ensures high $I_{ON}/I_{OFF}$ ratio and higher breakdown voltage.

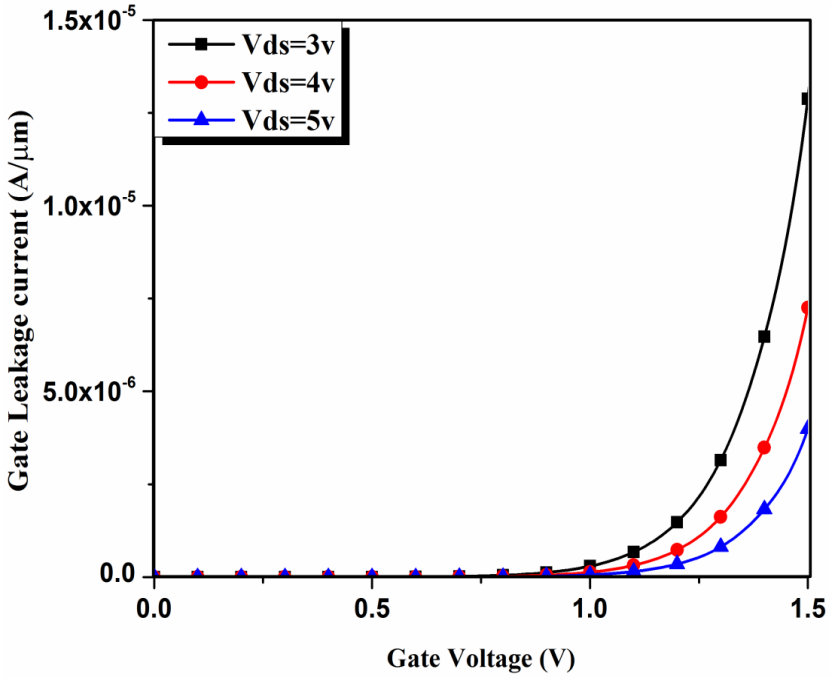


**Fig 3.4 Gate leakage current Vs. Gate voltage of T-gate n++GaN/InAlN/AlN/GaN Enhancement mode HEMT.**

### 3.2.5 RF PARAMETER ANALYSIS

In addition to the improved DC performance exhibited by the T-gate $n^{++}$ GaN/InAlN/ AlN/GaN Enhancement mode HEMT (discussed above), it is important to discuss the Analog/RF performance of this device. A comprehensive Analog/RF performance analysis would be useful to establish this device for high frequency and high power applications.

The $f_T$ is the frequency when the current gain is unity, whereas *fmax* is the frequency when the power gain is unity. $f_T$ is an important measure for high-speed digital applications (speed and high swing), while *fmax* corresponds to the transit frequency of the maximum available power gain (MAG), which is a realistic parameter for the optimization of high frequency amplifiers. Maximizing intrinsic gain, $f_T$ and *fmax* are the primary goals for RF applications. These two FOMs are given by [12]:

$$f_T = \frac{g_m}{2\pi C_{gs}\sqrt{1+2(C_{gd}/C_{gs})}} \approx \frac{g_m}{2\pi(C_{gd}+C_{gs})} \approx \frac{g_m}{2\pi C_{gg}} \qquad \textbf{(4.1)}$$

$$f_{max} = \frac{g_m}{2\pi C_{gs}\sqrt{(R_s+R_i+R_g)\left(g_{ds}+g_m\left(C_{gd}/C_{gs}\right)\right)}} \qquad \textbf{(4.2)}$$

where $g_m$ and $g_{ds}$ are the transconductance and output conductance, $R_g$, $R_s$, and $R_i$ are the gate, source and channel resistance respectively, $C_{gg}$ is the total gate capacitance which includes fringing capacitance.

Small signal AC analysis is performed over a wide frequency range using 2-D device simulator and Y-parameters are computed. Then, an advanced two port network RF extraction post processing tool is used to generate the different RF-FOMs ($f_T$ and *fmax*)

by converting admittances and capacitances to H-parameters as [13].

$$\mathbf{f_T = f_o \times |H21|} \quad \textbf{(4.3)}$$

$$f_{max} = f_o \sqrt{\frac{|Y_{21} - Y_{12}|^2}{4[Re(Y_{11})Re(Y_{22}) - Re(Y_{12})Re(Y_{21})]}} \quad \textbf{(4.4)}$$

where, $\mathbf{f_0}$ is the applied frequency **(1 MHz)** and $\mathbf{H_{21}}$ is the short circuit current gain.

RF performance of proposed device is plotted in Figure 3.5. Cut off frequency of **195 GHz**, and a maximum frequency of **110 GHz** is obtained. High cut off frequency is obtained due to suppression of SCE because of introducing T-Gate as here the introduced T-Gate is not recessed one.

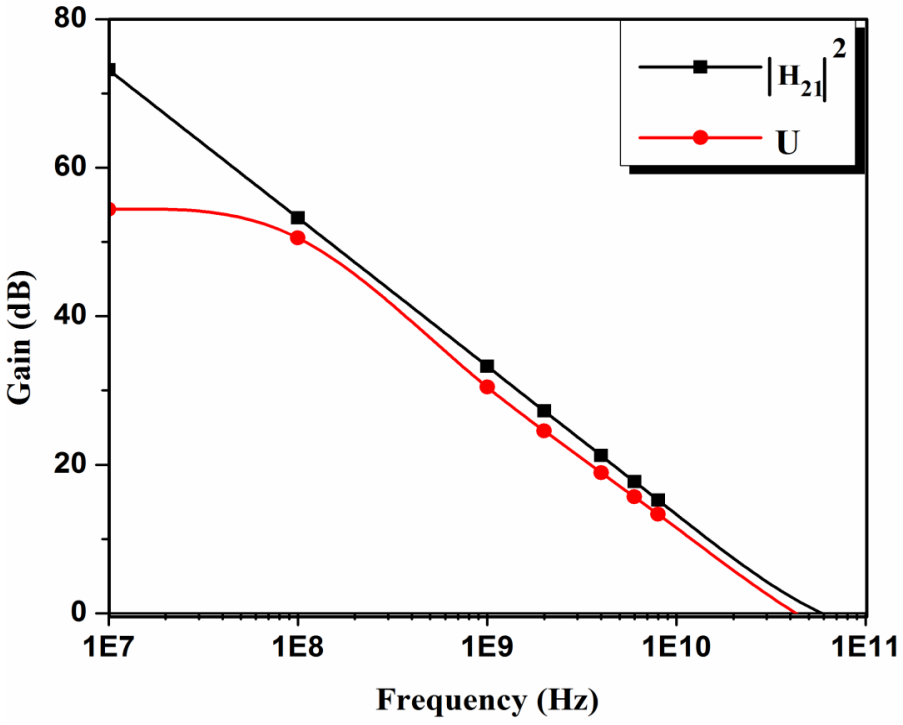


**Fig. 3.5 RF performance of T-gate $n^{++}$GaN/InAlN/AlN/GaN Enhancement mode HEMT.**

## 3.3 IMPACT OF $n^{++}$ GaN Cap Layer doping Variation

HEMTs based on an InAlN/GaN heterostructure system offer some additional advantage over the most conventional AlGaN/GaN counterparts due to higher polarization charge in the QW even without a strain in the barrier layer [14], [15] and extremely high thermal stability [16]. Nonexistence of the strain in the barrier has been shown to enhance the device reliability [17], while high polarization charge in the HEMT QW leads to high drain current density [16] and facilitates extreme scalability of the device [18]. It has been shown elsewhere for InAlN/GaN HEMTs that the undoped GaN capping does not affect the surface trap density, which is equal to the level of the counterpart polarization charge in the QW [19]. Thus, the GaN cap itself may not be considered as true passivation.

An increase in dynamical source access resistance ($dR_S$) with increased drain bias deteriorates transconductance ($g_m$), cutoff frequency ($f_T$), and even HEMT linearity [20]. The apparent early velocity saturation of electrons in the source access region due to the surface charging may explain the effect [21]. The $n^{++}$ GaN cap layer (6 nm thick) on AlGaN/GaN HEMTs has been shown to eliminate the $dR_S$ increase [22]. $n^{++}$ GaN was shown to also enhance dc HEMT parameters by reducing ohmic resistance ($R_s$) [23].

In this section, we focus on the effects related to the $n^{++}$ GaN capping layer, which turns out to be an important part of the structure. This section compares various DC and RF parameters of the proposed device such as transconductance, leakage current, transconductance generation factor, current Gain, power Gain for varying $n^{++}$ GaN cap

layer doping density. To the best of our knowledge, a detailed analysis of the effect of varying GaN cap layer density on the device performance of T-gate $n^{++}$GaN/InAlN/ AlN/GaN HEMT is not done yet. Thus, we have comprehensively analyzed the impact of n++ GaN cap layer density on device performance of T-gate $n^{++}$GaN/InAlN/AlN/GaN HEMT.

### 3.3.1 DRAIN CURRENT ANALYSIS

In the GaN cap, the profile reaches $N_{GaN} > 1\times10^{20}$ $cm^{-3}$. As expected, the free carriers in the 6-nmthick GaN cap are depleted from both sides, with the more pronounced depletion effect from the GaN/InAlN junction. The depletion in GaN from the side of InAlN is about twice that we expected for $N_{GaN} = 2\times10^{20}$ $cm^{-3}$. The pronounced depletion from the InAlN side is probably due to the high polarization charge at the GaN/InAlN junction. From the fig. 3.6 it is very clear that n++ GaN does effect the channel formed at the hetero interface and it provides lateral conduction in HEMTs.

Typical transfer characteristics of proposed 100nm T-gate $n^{++}$ GaN/InAlN/ AlN/GaN Enhancement mode HEMT but with varying $n^{++}$ GaN cap density have been plotted in Figure 3.6. As the concentration of Cap layer increases so does maximum value of drain current. A maximum drain current of 0.64A/mm is obtained at Vgs=2.0V for the cap doping density of 2E20 $cm^{-3}$ virtue of high mobility and velocity of 2DEG in the buried channel. High value of 2DEG density in the buried channel results in high drain current. Maximum drain current increases significantly with increase in Cap doping density as it participates in HEMT lateral conductivity.

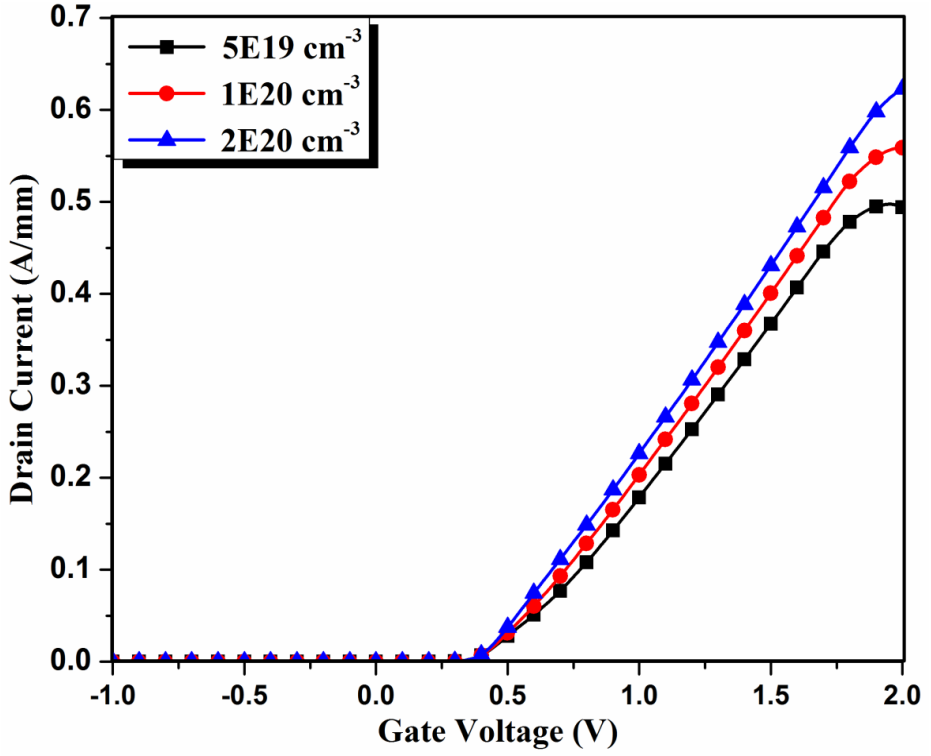


**Fig. 3.6 Simulated Transfer characteristics of T-gate $n^{++}$GaN/InAlN/AlN/GaN Enhancement mode HEMT, Lg=100nm.**

## 3.3.2 TRANSCONDUCTANCE VARIATION

**Transconductance** is the ratio of the change in drain current to the change in gate voltage over a defined, arbitrarily small interval on the drain-current-versus-gate-voltage curve. Transconductance (for transfer conductance), also infrequently called as mutual conductance, is the electrical characteristic relating the current through the output of a device to the voltage across the input of a device. Figure 3.7 represents transconductance variation with $V_{gs}$ for the proposed device. Here, it is observed that at a GaN cap doping density of 2E20 $cm^{-3}$ a peak transconductance of 437.5 mS/mm is achieved. Broader $g_m$ profile provides an improved linear behavior from which a smaller

intermodulation distortion, a smaller phase noise and a larger dynamic range could be expected [11]. Variation in transconductance is observed from the simulated graph and it is mainly because of change in polarization because of change in GaN doping density.

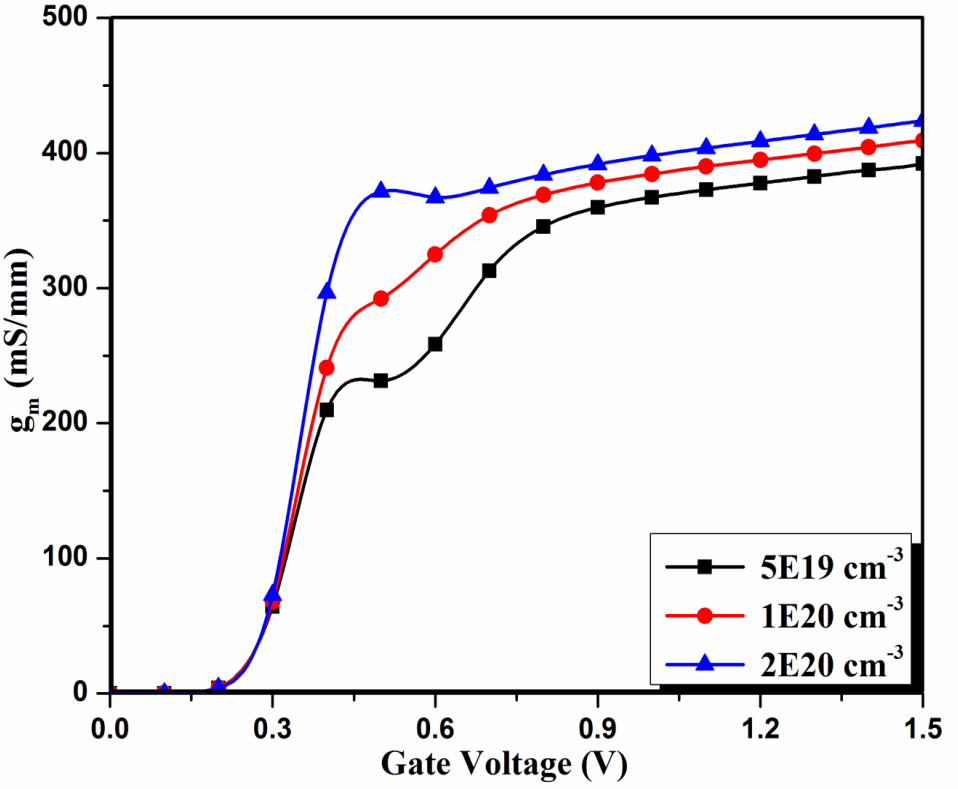


**Fig. 3.7 Simulated transconductance curve of T-gate $n^{++}$GaN/InAlN/AlN/GaN Enhancement mode HEMT.**

## 3.3.3 TRANSCONDUCTANCE GENERATION FACTOR

Transconductance-to-current ratio ($g_m/I_d$) also known as the transconductance generation factor (TGF) is a key figure of merit in the design of subthreshold low-power analog applications [11]. TGF can be defined as the available gain per unit value of power dissipation, because $g_m$ represents the gain, and $I_d$ represents the power dissipated to

obtain that amplification. Lower TGF implies decreased input drive ability and hence, higher power dissipation in capacitive load circuits. TGF as a function of variable GaN cap density is shown in figure 3.8. A very high value of 212 $V^{-1}$ is obtained at cap layer of 2E20 $cm^{-3}$. This high value of TGF achieved is utilized in analog applications. TGF attains peak value at low gate bias and degrades severely at higher gate bias, due to increased value of $I_d$ at higher $V_{gs}$.

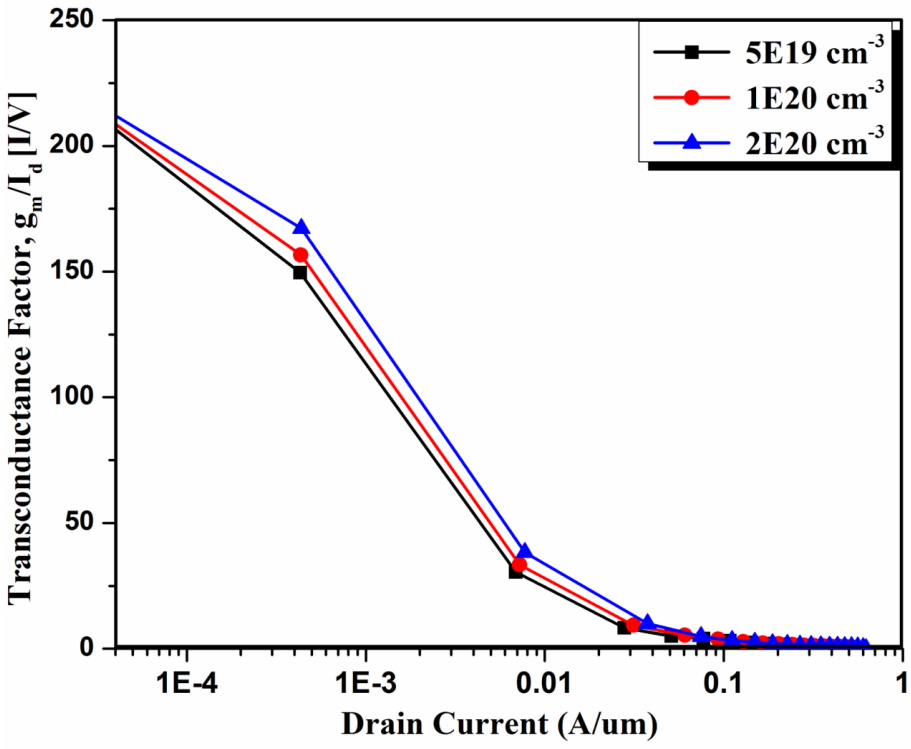


**Fig. 3.8 Dependence of Transconductance generation factor ($g_m/I_d$) on Drain Current.**

## 3.3.4 GATE LEAKAGE CURRENT

As the continuous down-scaling of the device size has led to very thin gate oxides, the leakage current that can flow from the channel to the gate comes into the

order of the subthreshold leakage current and the gate cannot be considered as an ideally insulated electrode anymore. This affects the circuit functionality and increases the standby power consumption due to the static gate current. Even though we are simulating our device at room temperature, Poole-Frenkel emission component has been only considered for Gate leakage Current. Gate leakage current Vs. Gate voltage has been plotted in Figure 3.9 for the proposed device and is in the order of $10^{-5}$ as observed from the plot which is very low due to introduction of T-Gate. Low gate leakage current ensures high $I_{ON}/I_{OFF}$ ratio and higher breakdown voltage. With increase in $n^{++}$ GaN cap doping gate leakage current considerably increases which is mainly due to increase in induced polarization.

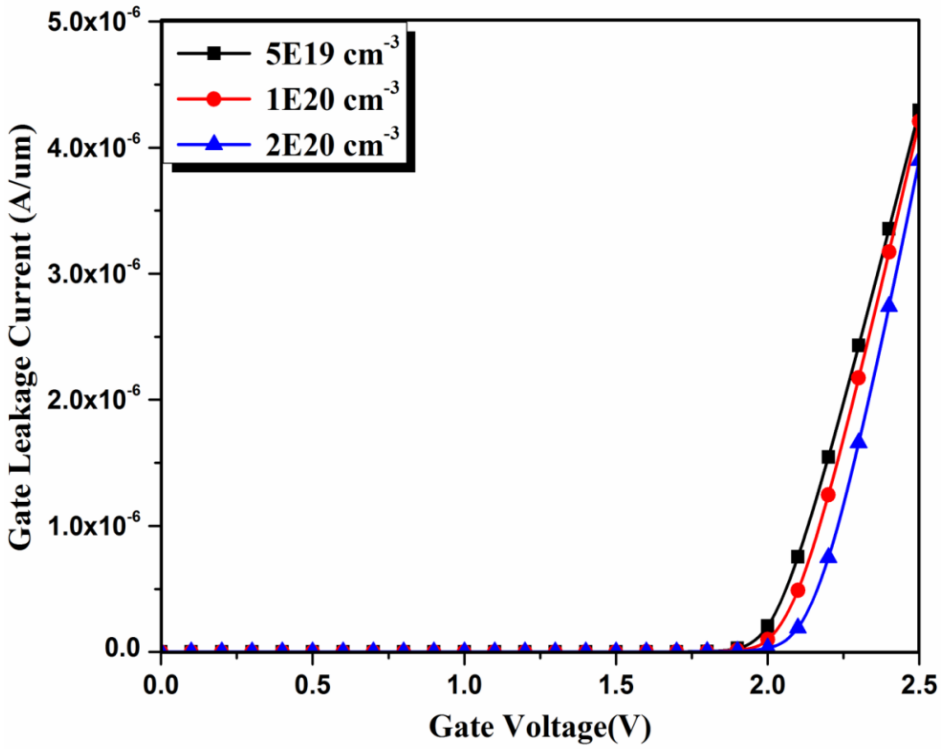


**Fig 3.9 Gate leakage current Vs. Gate voltage of T-gate n++GaN/InAlN/AlN/GaN Enhancement mode HEMT.**

### 3.3.5 POWER AND CURRENT GAIN

In electronics, gain is a measure of the ability of a two port circuit (often an amplifier) to increase the power or amplitude of a signal from the input to the output port by adding energy converted from some power supply to the signal. It is usually defined as the mean ratio of the signal amplitude or power at the output port to the amplitude or power at the input port. It is often expressed using the logarithmic decibel (dB) units ("dB gain"). Gain greater than one (zero dB), that is amplification, is the defining property of an active component or circuit, while a passive circuit will have a gain of less than one.

Power Gain vs. frequency is plotted in figure 3.10. The graph shows gain decreases with increase in GaN cap density. The graph confirms that the said device can be used as amplifier upto the order of 1E11 Hz.

Current Gain vs frequency plot has been shown in figure 3.11. The gain decreases with increase in GaN cap doping density. With increase in density the frequency range of the device also increases. Hence the said device can be utilized as amplifier upto a large frequency range with increased doping. The current gain sets an upper limit to the fan-out of the logic gate.

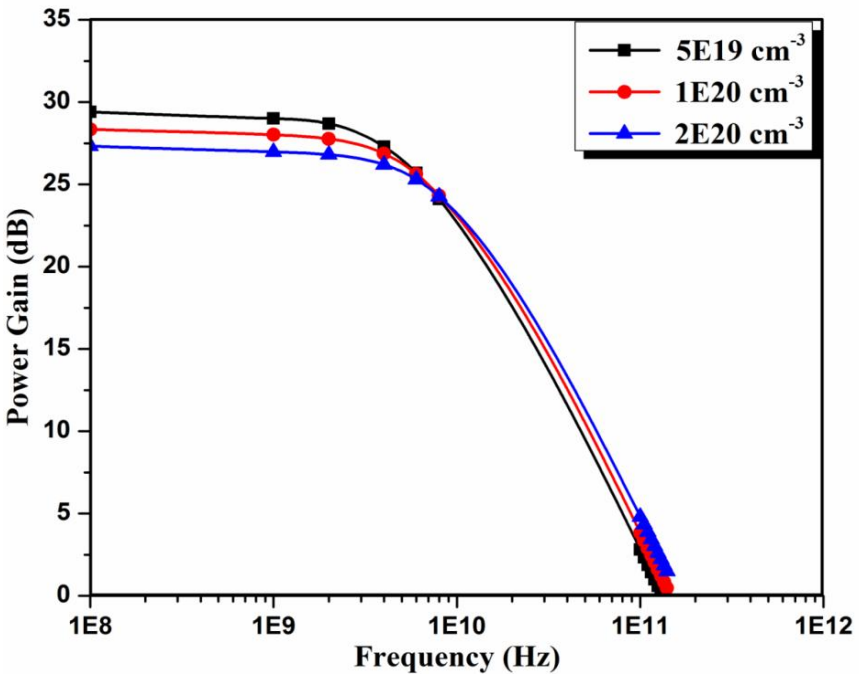


**Fig. 3.10 RF performance of T-gate $n^{++}$GaN/InAlN/AlN/GaN Enhancement mode HEMT.**

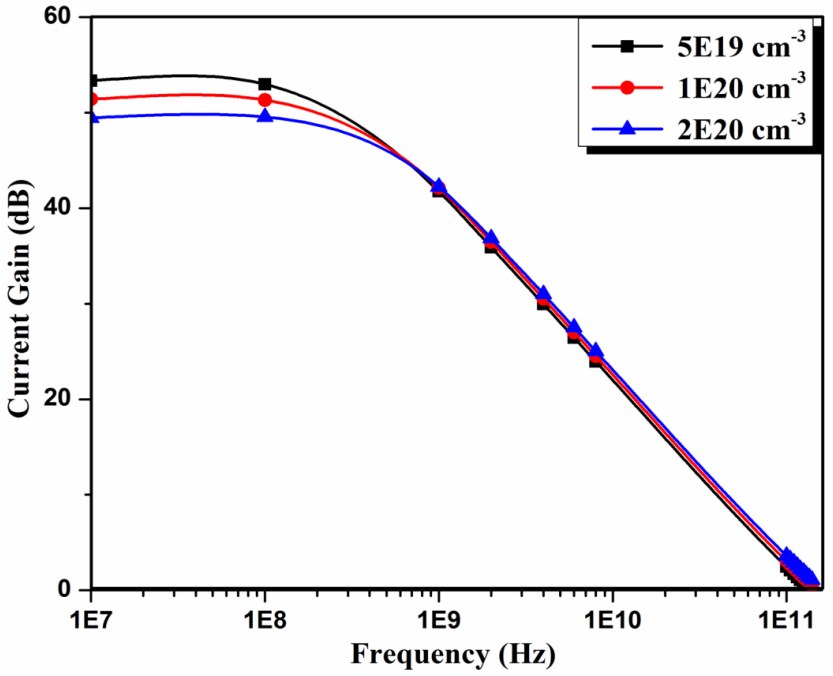


**Fig. 3.11 RF performance of T-gate $n^{++}$GaN/InAlN/AlN/GaN Enhancement mode HEMT.**

## Summary:

The chapter discusses the effect of Drain voltage variation and $n^{++}$ GaN cap doping on various parameters of the device. Variation in Drain current, Transconductance, Transconductance generation factor (TGF), Power Gain, Current Gain, $f_T$, $f_{max}$, gate leakage current has been extensively discussed. Introduction of T-gate in the already proposed enhancement mode $n^{++}$ GaN/InAlN/AlN/GaN HEMT results in high drain current, low leakage current, reduced SCE, high $I_{ON}/I_{OFF}$ ratio, high Transconductance Generation Factor (TGF), and high $f_T$ and $f_{max}$ which can be utilized in high frequency switching application and even can be utilized in Analog and RF mixed signal applications.

## References

[1] R. Wang, P. Saunier, X. Xing, C. Lian, X. Gao, S. Guo, G. Snider, P. Fay, D. Jena, and H. Xing, "Gate-recessed enhancement-mode InAlN/AlN/GaN HEMTs with 1.9 A/mm drain current density and 800 mS/mm transconductance," IEEE Electron Device Lett., vol. 31, no. 12, pp. 1383–1385, Dec. 2010.

[2] B. Song, B. Sensale-Rodriguez, R. Wang, A. Ketterson, M. Schuette, E. Beam, et al., "Monolithically integrated E/D-mode InAlN HEMTs with $f$t /$f$max > 200/220 GHz," in Proc. IEEE 70th Annu. DRC, Jun. 2012, pp. 1–2.

[3] B. Song, B. Sensale-Rodriguez, R. Wang, J. Guo, Z. Hu, Y. Yue, F. Faria, M. Schuette, A. Ketterson, E. Beam, P. Saunier, X. Gao, S. Guo, P. Fay, D. Jena, H.G.Xing, "Effect of Fringing Capacitances on the RF Performance of GaN HEMTs With T-Gates," IEEE Trans Elec. Dev.,, vol.61, no.3, pp.747-754, March 2014.

[4] G. H. Jessen, R. C. Fitch, J. K. Gillespie, G. Via, A. Crespo, D. Langley, D. J. Denninghoff, M. Trejo, and E. R. Heller, "Short-channel effect limitations on high-frequency operation of AlGaN/GaN HEMTs for T- Gate devices," IEEE Trans. Electron Devices, vol. 54, no. 10, pp. 2589–2597, Oct. 2007.

[5] S. Adak, A. Sarkar, S. Swain, H. Pardeshi, S.K. Pati, C.K. Sarkar, "High performance AlInN/AlN/GaN p-GaN back barrier Gate-Recessed Enhancement-Mode HEMT" Superlattices and Microstructures, vol. 75, pp. 347-357 ,2014.

[6] D. M. Geum et al., "75 nm T-shaped gate for In0.17Al0.83N/GaN HEMTs with minimal short-channel effect," Electron. Lett., vol. 49, no. 24, pp. 1536–1537, Nov. 2013.

[7] Liu Bo , Feng Zhihong , Dun Shaobo , Zhang Xiongwen ,Gu Guodong , Wang Yuangang , Xu Peng , He Zezhao and Cai Shujun. An extrinsic fmax > 100 GHz InAlN/GaN HEMT with AlGaN back barrier. Journal of Semiconductors, 2013, 34(4): 044006.

[8] R. Chau, S. Datta and A. Majumdar, "Opportunities and Challenges of III-V Nanoelectronics for Future High-Speed, Low-Power Logic Applications," *Compound Semiconductor Integrated Circuit Symposium-2005*, pp. 17-20, 2005.

[9] T. Kachi, in Proceedings of IEEE Compound Semiconductor IC Symposium, San Francisco, CA, USA, October 16–19, 2007, pp.13.

[10] Tsividis Y, Operation and modelling of the MOS Transistor, 2nd edition Boston: McGraw-Hill (1999).

[11] E. Vittoz, J. Fellrath, "CMOS Analog Integrated Circuits Based on Weak Inversion Operation," *IEEE Journal of Solid-State Circuits*, vol. SC-12 , no. 3, pp. 224–231, 1977.

[12] D. Flandre, J. P. Raskin, D. Vanhoenacker, "SOI CMOS Transistors for RF and Microwave Applications," *International Journal of High Speed Electron System*, vol. 11, no. 4, pp. 1159–1248, 2001.

[13] N. Mohankumar, B. Syamal, C. K. Sarkar, "Influence of Channel and Gate Engineering on the Analog and RF Performance of DG MOSFETs," *IEEE Transaction on Electron Devices*, vol. 57, no. 4, pp. 820–826, 2010.

[14] J. Kuzmik, "InAlN/(In)GaN high electron mobility transistors: Some aspects of the quantum well heterostructure proposal,"Semicond. Sci.Technol., vol. 17, no. 6, pp. 540–544, Jun. 2002.

[15] M. Gonschorek, J.-F. Carlin, E. Feltin, M. A. Py, N. Grandjean, V. Darakchieva, B. Monemar, M. Lorenz, and G. Ramm, "Twodimensional electron gas density in Al1−xInxN/AlN/GaN heterostructures (0.03≤x≤0.23)," J. Appl. Phys., vol. 103, no. 9, p. 093 714, May 2008.

[16] F. Medjdoub, J.-F. Carlin, M. Gonschorek, E. Feltin, M. A. Py, D. Ducatteau, C. Gaquière, N. Grandjean, and E. Kohn, "Can InAlN/GaN be an alternative to high power/high temperature AlGaN/GaN devices" in IEDM Tech. Dig., 2006, pp. 1–4.

[17] J. Kuzmik, G. Pozzovivo, C. Ostermaier, G. Strasser, D. Pogany, E. Gornik, J.-F. Carlin, M. Gonschorek, E. Feltin, and N. Grandjean, "Analysis of degradation mechanisms in lattice-matched InAlN/GaN high-electron-mobility transistors," J. Appl. Phys., vol. 106, no. 12, p. 124 503, Dec. 2009.

[18] F. Medjdoub, M. Alomari, J.-F. Carlin, M. Gonschorek, E. Feltin, M. A. Py, N. Grandjean, and E. Kohn, "Barrier-layer scaling of InAlN/GaN HEMTs,"IEEE Electron Device Lett., vol. 29, no. 5, pp. 422–425, May 2008.

[19] J. Kuzmik, J.-F. Carlin, M. Gonschorek, A. Kostopoulos, G. Konstantinidis, G. Pozzovivo, S. Golka, A. Georgakilas, N. Grandjean, G. Strasser, and D. Pogany, "Gate-lag and drain-lag effects in (GaN)/InAlN/GaN andInAlN/AlN/GaN HEMTs,"Phys. Stat. Sol. (A), vol. 204, no. 6, pp. 2019–2022, Jun. 2007.

[20] Palacios, S. Siddharth, A. Chakroborty, S. Heikmann, S. Keller, S. P. DenBaars, and U. K. Mishra, "Influence of the dynamic access resistance in the $g_m$ and $f_T$ linearity of AlGaN/GaN HEMTs," IEEE Trans. Electron Devices, vol. 52, no. 10, pp. 2117–2123, Oct. 2005.

[21] Y. Pei, L. Shen, T. Palacios, N. A. Fichtenbaum, L. S. McCarthy, S. Keller, S. P. DenBaars, and U. K. Mishra, "Study of the n+ GaN cap in AlGaN/GaN high electron mobility transistors with reduced source drain resistance" J pn. J. Appl. Phys., vol. 46, no. 35, pp. L842–L844, 2007.

# *Chapter 4*

# PERFORMANCE ANALYSIS FOR VARYING GATE LENGTH

## 4.1 INTRODUCTION

The gate length ($L_g$) is a key factor that determines the device performance of MOS-HEMT. Few groups have analyzed the effect of these parameters on the device performance. Lee. Et.al. investigated the influence of $L_g$ on drain current, Delay, $f_T$, $f_{max}$ for the InAlN /GaN HEMTs [1]. Wang.et.al analyzed the effect of $L_g$ and barrier thickness scaling on DC and RF performance of InAlN/GaN HEMT [2]. Gaquiere et.al. Analyzed the effect of $L_g$ on DC and RF characteristics for AlInN/GaN HEMT [3]. The ensemble Monte Carlo 2D simulation of AlInN/InGaN/AlInN double heterojunction FET was done to analyze the DC and RF performance for varying $L_g$ [4]. Many groups have reported the growth and characteristics of fixed length $Al_{0.83}In_{0.17}N$/GaN HEMT devices [5-14].

Monte Carlo simulation of GaN based HEMT for variation in source-gate (S-G) and gate-drain (G-D) distance showed that a downscaling of the S-G distance can improve the device performance, enhances the output current and the device transconductance; on the contrary, the gate-drain distance does not affect the output current [15]. In buried channel devices such as HEMT and MOS-HEMT, higher aspect ratio (ratio of gate length and effective dielectric thickness separating the gate and channel) is desirable for enhancing the high frequency performance [16]. As $L_g$ is scaled, the aspect ratio decreases and degrades the RF performance. High aspect ratio is also necessary to minimize SCEs, as SCE are highly detrimental to RF performance in these devices [17]. Here we have comprehensively analyzed the effect of gate length on device

performance of T-gate $n^{++}$GaN/InAlN/AlN/GaN HEMT. Extensive device simulations of the major device performances indicators such as $I_d$, $g_m$, $g_m/I_d$, Gate leakage current, $f_T$, $f_{max}$ have been done for wide range of $L_g$.

## 4.2 IMPACT OF GATE LENGTH

Due to scaling, gate length of MOSFETs is continuously shrinking, making it imperative to analyze the impact of $L_g$ on the device performance. The device structure (Fig. 2.11) and the calibrated simulation model discussed in chapter 2 are used in this analysis. The $L_g$ is varied from 75nm to 125nm.

### 4.2.1 DRAIN CURRENT ANALYSIS

Fig 4.1 shows the transfer characteristics of the T-gate $n^{++}$GaN/InAlN/AlN/GaN HEMT for variable $L_g$ ranging from 75nm to 125nm. As seen from the Fig 4.1 a very high drain current density of 0.87 A/mm is obtained for device having $L_g$ = 75nm. This is because of the high mobility and velocity of 2DEG in the channel. In addition, high value of 2DEG density in the channel results in high drain current. For lower bias, the drain current (linear drive current) is proportional to conductivity of the channel and for higher bias, the drain current (saturated drive current) is proportional to carrier density and carrier injection velocity. The carrier injection velocity in turn is a function of low-field carrier mobility and effective mass ($m_n$) [18]. As observed from the transfer characteristics, drain current is inversely proportional to channel length ($L_g$). The drain current increase as $L_g$ reduces due to increase in channel resistance.

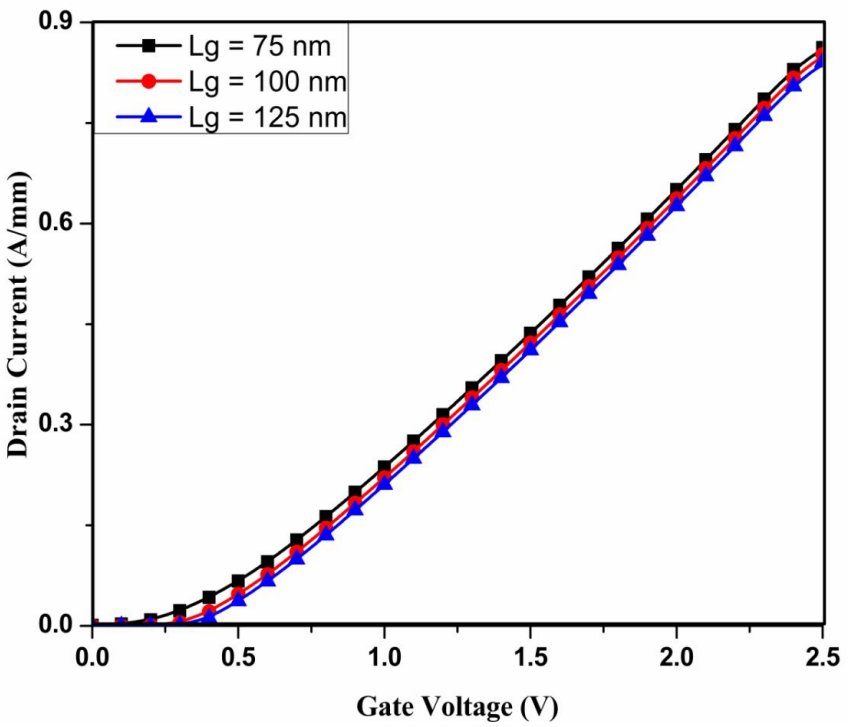


**Fig. 4.1 $I_d$ versus $V_g$ characteristics for applied drain voltage $V_{ds}$=3V. $L_g$ is varied from 75 nm to 125 nm.**

### 4.2.2 TRANSCONDUCTANCE VARIATION

Transconductance can be obtained from the ratio of variation in $I_d$ to the variation of gate voltage ($V_{gs}$), for constant drain voltage ($V_{ds}$) [19]. Fig 4.2 shows the influence of $L_g$ on the transconductance as a function of Gate voltage. Transconductance is observed to be increase at lower gate bias but gets saturated at higher $V_{gs}$ because of saturation polarization. The increase in current (and therefore $g_m$) can be evaluated as a function of the charge (n) and the velocity (v) increments. By Elena et. Al. [20] it was found that $\Delta n.vx$ term has the highest contribution to the current variation, while the other terms have a negligible impact. In particular, $\Delta n$ (increment in charge) variation is more for $L_g$ variation, thus explaining the increase of $g_m$ and $I_d$ for reduction in $L_g$. Decrease in $g_m$ with the

increase in $L_g$ is due to increase in channel resistance which restricts the $g_m$. . Because of polarization effect a very minute variation is observed in transconductance peak for varying drain bias. Here, it is observed that at a gate voltage of 2.0 V a peak transconductance of 442.5 mS/mm is achieved at a gate length of 75 nm. Broader $g_m$ profile provides an improved linear behavior from which a smaller intermodulation distortion, a smaller phase noise, and a large dynamic range could be expected [21].

### 4.2.3 TRANSCONDUCTANCE GENERATION FACTOR

Transconductance-to-current ratio ($g_m/I_d$) also known as the transconductance generation factor (TGF) is a key figure of merit in the design of subthreshold low-power analog applications [22]. Lower TGF implies decreased input drive ability and hence, higher power dissipation in capacitive load circuits. TGF can be defined as the available gain per unit value of power dissipation, because $g_m$ represents the gain, and $I_d$ represents the power dissipated to obtain that amplification. TGF as a function of $V_{gs}$ for variable Gate length is shown in figure 4.3. TGF has a peak at lower $V_{gs}$ and degrades severely at higher $V_{gs}$, due to increased value of $I_d$ at higher $V_{gs}$. As $L_g$ decreases, short channel effects start to dominate, and thereby TGF falls appreciably. Also we know $I_d$ increases due to reduced channel resistance as $L_g$ decreases, which eventually lead to decrease in $g_m/I_d$ ratio. Here the peak TGF value observed is 147.51 $V^{-1}$ for device having $L_g$ = 125nm.

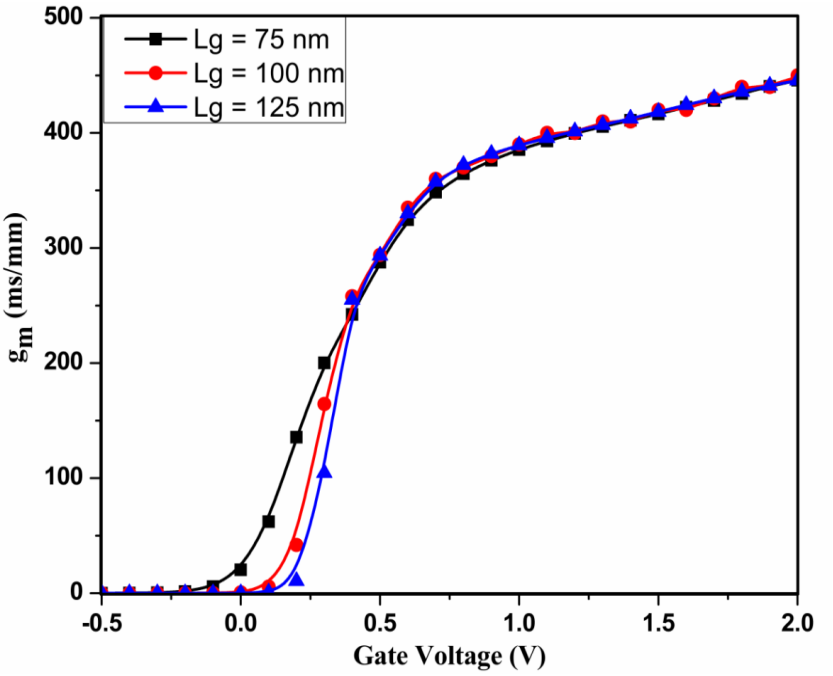


**Fig. 4.2 Simulated transconductance curve of T-gate $n^{++}$GaN/InAlN/AlN/GaN Enhancement mode HEMT. $L_g$ is varied from 75nm to 125 nm.**

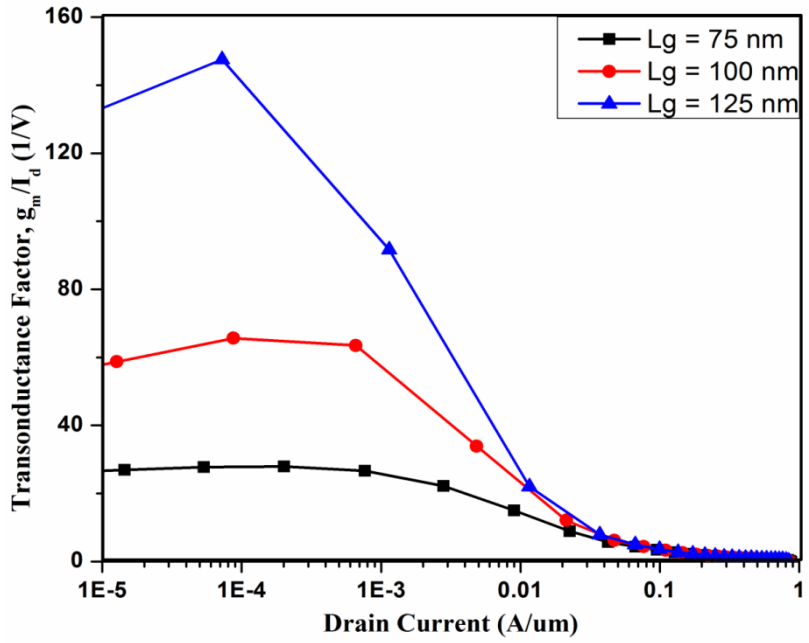


**Fig. 4.3 Dependence of Transconductance generation factor ($g_m/I_d$) on Drain Current. $L_g$ is varied from 75 nm to 125 nm.**

## 4.2.4 GATE LEAKAGE CURRENT

With the continuous shrinking of device size has led to very thin gate oxides, which results in leakage current of the order of subthreshold leakage current that can flow from the channel to the gate and hence the gate cannot be considered as an ideally insulated electrode anymore. This affects the circuit functionality and increases the standby power consumption due to the static gate current.

Even though we are simulating our device at room temperature, Poole-Frenkel emission component has been only considered for Gate leakage Current. Gate leakage current Vs. Gate voltage has been plotted in Figure 4.4 for the proposed device and is in the order of $10^{-5}$ as observed from the plot which is very low due to introduction of T-Gate. Low gate leakage current ensures high $I_{ON}/I_{OFF}$ ratio and higher breakdown voltage.

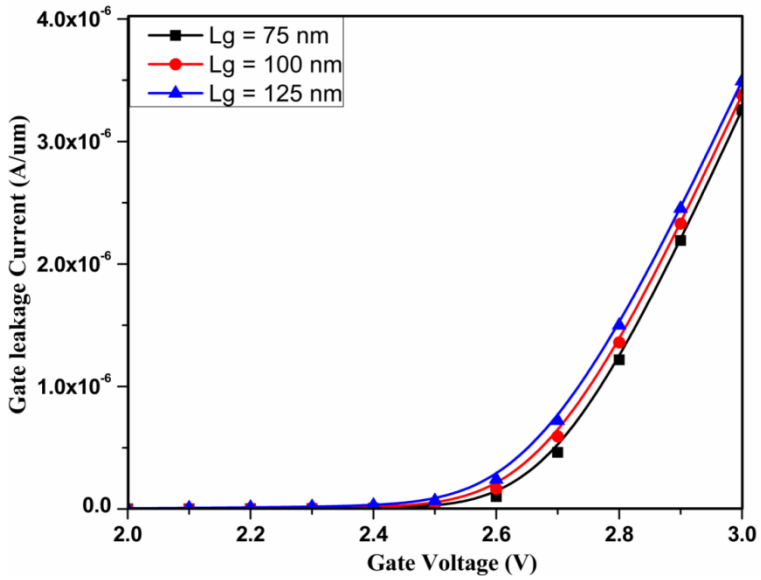


**Fig 4.4 Gate leakage current Vs. Gate voltage of T-gate $n^{++}$ GaN/InAlN/AlN/GaN Enhancement mode HEMT. Gate Length is varied from 75nm to 125 nm.**

## Summary:

In this chapter RF performance is analyzed for a wide range of $L_g$, using 2D Sentaurus TCAD simulation. The simulation is done using Hydrodynamic model. The parameters analyzed include Drain current, Transconductance, Transconductance generation factor (TGF), $f_T$, $f_{max}$. The reduction of $L_g$ leads to increase in $I_{d,}$ whereas Gate leakage current, TGF, $g_m$ decreases. Introduction of T-gate in the already proposed enhancement mode $n^{++}$ GaN/InAlN/AlN/GaN HEMT results in high drain current, low leakage current, reduced SCE, high $I_{ON}/I_{OFF}$ ratio, high Transconductance Generation Factor (TGF), and high $f_T$ and $f_{max}$ which can be utilized in high frequency switching application and even can be utilized in Analog and RF mixed signal applications. The device parameters can be selected appropriately for achieving desired performance.

## References

[1] Dong Seup Lee, Xiang Gao, Shiping Guo, et.al., "300-GHz InAlN/GaN HEMTs with InGaN Back Barrier," *IEEE Electron Device Letters*, vol. 32, no. 11, pp. 1325-1527, 2011.

[2] H. Wang, J. W. Chung, X. Gao, et.al., "High Performance InAlN/GaN HEMTs on SiC Substrate," in *CS Mantech- 2010*, pp. 185-188, 2010.

[3] C. Gaquiere, F. Medjdoub, J. F. Carlin, et.al., "AlInN/GaN a suitable HEMT device for extremely high power high frequency applications," in : *International Microwave Symposium-2007*, pp. 2145- 2148, 2007.

[4] Kazuki Kodama and Masaaki Kuzuhara, "Theoretical simulation of DC and RF performance for AlInN/InGaN/AlInN double-heterojunction FET using a Monte Carlo approach," *IEICE Electronics Express*, vol. 5, no. 24, pp. 1074-1079, 2008.

[5] L. R. Khoshroo, C. Mauder, W. Zhang, et.al., "Optimization of AlInN/GaN HEMT structures," *Physica Status Solidi-C,* vol. 5, no. 6, pp. 2041-2043, 2008.
[6] A. Dadgar, F. Schulze, and A. Diez, "High sheet charge carrier density AlInN/GaN field-effect transistors on Si (111)," *Applied Physics Letters,* vol. 85, no. 22, pp. 5400-5404, 2004.
[7] C. Ostermaier, G. Pozzovivo, J. François Carlin, et.al., "Ultrathin InAlN/AlN Barrier HEMT with high performance in Normally-Off operation," *IEEE Electron Device Letters,* vol. 30, no. 10, pp. 1030-1032, 2009.
[8] B. Liu, Z. Feng, S. Zhang, et.al., "A 4.69-W/mm output power density InAlN/GaN HEMT grown on sapphire substrate," *Journal of Semiconductors,* vol. 32, no. 12, pp. 124003-1 - 124003-4, 2011.
[9] H. W. Barrier, A. Crespo, M. M. Bellot, et.al., "High-Power Ka-Band performance of AlInN/GaN," *IEEE Electron Device Letters,* vol. 31, no. 1, pp. 8-10, 2010.
[10] N. Sarazin, E. Morvan, M. A. F. Poisson, et.al., "AlInN/AlN/GaN HEMT technology on SiC with 10-W/mm and 50% PAE at 10 GHz," *IEEE Electron Device Letters,* vol. 31, no. 1, pp. 11-14, 2010.
[11] H. Sun, A. R. Alt, H. Benedickter, et.al., "205-GHz (Al,In)N/GaN HEMTs," *IEEE Electron Device Letters,* vol. 31, no. 9, pp. 957-959, 2010.
[12] H. Sun, A. R. Alt, H. Benedickter, et.al., "102-GHz AlInN/GaN HEMTs on silicon with 2.5-W/mm output power at 10 GHz," *IEEE Electron Device Letters,* vol. 30, no. 8, pp. 796-798, 2009.
[13] Q. Zhou, D. Marti, H. Sun, et.al., "Fully Passivated AlInN/GaN HEMTs with $f_T/f_{max}$ of 205/220 GHz," *IEEE Electron Device Letters,* vol. 32, no. 10, pp. 1364-1366, 2011.
[14] X. Ni. Xie, M. Wu, et.al., "High electron mobility in nearly lattice-matched AlInN/AlN/GaN heterostructure field effect transistors," *Applied Physics Letters,* vol. 91, pp. 132116-1 - 132116-3, 2007.

[15] Stefano Russo and Aldo Di Carlo, "Influence of the Source–Gate distance on the AlGaN/GaN HEMT performance," *IEEE Transactions on Electron Devices*, vol. 54, no. 5, pp. 1071-1075, 2007.

[16] Y. Awano, M. Kosugi, K. Kosemura, et.al., "Short-channel effects in subquarter-micrometer gate HEMTs: simulation and experiment," *IEEE Transactions on Electron Devices*, vol. 36, no. 10, pp. 2260-2265, 1989.

[17] Gregg H. Jessen, Robert C. Fitch, James K. Gillespie, et.al., "Short-Channel effect limitations on high-frequency operation of AlGaN/GaN HEMTs for T-Gate devices," *IEEE Transactions on Electron Devices*, vol. 54, no. 10, pp. 2589-2597, 2007.

[18] R. Chau, S. Datta and A. Majumdar, "Opportunities and Challenges of III-V Nanoelectronics for Future High-Speed, Low-Power Logic Applications," *Compound Semiconductor Integrated Circuit Symposium-2005*, pp. 17-20, 2005.

[19] Tsividis Y, Operation and modelling of the MOS Transistor, 2nd edition Boston: McGraw-Hill (1999).

[20] Elena Pascual, Raúl Rengel and María J. Martín, "Influence of the underlap length on the RF noise performance of a Schottky Barrier MOSFET," in: *Proceedings of 21st International Conference on Noise and Fluctuation -2011*, pp. 230-233, 2011.

[21] M. A. Khan, X. Hu, G. Simin, et.al., "AlGaN/GaN metal oxide semiconductor heterostructure field effect transistor," *IEEE Electron Device Letters*, vol. 21, no. 2, pp. 63-65, 2000.

[22] E. Vittoz, J. Fellrath, "CMOS Analog Integrated Circuits Based on Weak Inversion Operation," *IEEE Journal of Solid-State Circuits*, vol. SC-12 , no. 3, pp. 224–231, 1977.

# *Chapter 5*

# CONCLUSION

# AND

# FUTURE SCOPE

## 5.1 CONCLUSION

The use of GaN based heterostructure (InAlN/GaN) in MOS-HEMT is increasing because of its material advantage such as wider $E_g$, higher operating temperature, higher $V_{Br}$, higher mobility, and higher saturation velocity. The most specular feature in GaN based heterostructure is the two fold polarization (spontaneous and piezoelectric) responsible for high 2DEG sheet carrier density. Lattice matching in $Al_{0.83}In_{0.17}N$ heterostructure reduces strain related issues and thereby surface scattering. It offers positive aspects such as high 2DEG sheet carrier density making it a potential candidate for microwave power applications. These attributes have prompted us to use InAlN/GaN heterostructure for our proposed T-Gate Enhancement mode $n^{++}$ GaN/InAl N/AlN/GaN HEMT device.

T-gate structure is a solution to achieve the desired high frequency performance. Here the introduced T-gate is not recessed one so it overcomes the major SCE restrictions. T-gate technology is used to improve the device characteristics by reducing the gate resistance at very small gate length. The width of the T-gate head must be chosen optimally as a trade-off value between resistance and capacitance.

In this work the performance of proposed T-Gate Enhancement mode $n^{++}$ GaN/InAl N/AlN/GaN HEMT is comprehensively analyzed using 2D Sentaurus TCAD simulation for a wide range of device parameters. The proposed device results in higher drain current, low leakage current and reduced SCE high $I_{ON}/I_{OFF}$ ratio, high

Transconductance Generation Factor (TGF), and high $f_T$ and $f_{max}$. Because of these attributes it can be utilized in Analog and RF mixed signal application.

## 5.2 FUTURE SCOPE

Although the result obtained in this research work have demonstrated the potentials of Gate Enhancement mode $n^{++}$ GaN/InAl N/AlN/GaN HEMT, some issues remains to be investigated, and some new approaches may be worth pursuing to further improve the device performance. Some of the following future work could be :

- The actual fabrication of $n^{++}$ GaN/InAl N/AlN/GaN HEMT could be done, to provide further insight in the utility of such device for microwave based applications.
- As the proposed device is an E-mode device which offers positive threshold voltage so it can be utilized for further digital switching based applications.
- An understanding of defects and traps in this structure is essential for improving material quality and consequently device high frequency performance.